

People's Democratic Republic of Algeria
Ministry of Higher Education and Scientific Research
University M'Hamed BOUGARA – Boumerdes



Institute of Electrical and Electronic Engineering
Department of Electronics

Final Year Project Report Presented in Partial Fulfillment of
the Requirements for the Degree of

MASTER
In Telecommunication
Option: **Telecommunications**

Title:

Design and Simulation of a Novel Highly
performant Low Pass Filter

Presentedby:

- **HENDOU Sidahmed**
- **BOUALIA Mohamed**

Supervisor:

Prof.M.CHALLAL

Registration Number:...../2019

Abstract

This work presents a study and design of a microstrip low pass filter (LPF), The proposed LPF has acceptable performances in terms of insertion loss, high return loss in the pass-band, wide stop-band at 20 dB suppression level ranging from 1.78 GHz to more than 20 GHz and size of 40x18mm² compared to previous published works.

Keywords: LPS, DGS, Insertion loss, rejection.

ACKNOWLEDGEMENT

Before all, we would like to thank Allah “almighty” who gave us, health, courage and faith to complete our work.

First, we would like to thank our supervisor Mr. M. CHALLAL for his supervision, availability, fruitful remarks and precious guidance during our study and realization of this project.

we would also like to thank Dr. F. MOUHOUCHE for her help; finally, thanks to all IGEE lecturers for their huge efforts to groom future engineers and of course without forgetting the library staff.

We extend our thanks to the jury members who we have honored by evaluating, reviewing and enriching our modest work.

We are deeply indebted to our family and all friends for their valuable support and encouragements.

Dedication

I dedicate this modest work:

My beloved parents Mohamed and Djamila, my words are not enough to express my thanks to you, who continually provide their moral, spiritual emotional support and more.

To my sisters (especially my littles Manel and Souhila).

To all my beloved friends (Farouk, Rabah, Oussama, Housseyn and Walid)

And all my dearest friends.

To my teachers and classmates who shared their words of advice and encouragement.

To all the people in my life who touch my heart.

And lastly, I thank Allah for the guidance, strength, power of mind, protection and skills and for giving me a healthy life.

Sidahmed

Dedication

I dedicate this project to “ALLAH” Almighty my creator, my strong pillar, my source of inspiration, wisdom, knowledge and understanding.

I also dedicate this work to my parents whom have encouraged me all the way and whose encouragement have made sure that I give it all it

takes to finish that which I have started.

To my friends specially whom walked with me for five years or more,

Zakaria, Mohamed, Miloud, Rabah, Walid, Oussama & Houssine. For

everyone helped me to walk in my success road.

To all who read this final year project report

Mohamed

Table of Content

Abstract	I
Acknowledgement	II
Dedication.....	III
Table of Content.....	V
List of Tables	IX
List of Figures.....	X
List of Abbreviation	XII
List of Symbols	XIII
General Introduction	1
CHAPTER I: Filter Theory and Defected ground structure techniqueI.1	
Introduction.....	2
I.2 Expressions used in filters	2
I.2.1 Transfer function	2
I.2.2 Insertion loss	2
I.2.3 Return loss	3
I.2.4 Pass-band	3
I.2.5 Cutoff frequency	3
I.2.6 Stop band	3
I.2.7 Sharpness factor	3
I.3 RF/Microwaves filters’ classification.....	3
I.3.1 Low pass Filter (LPF).....	3
I.3.2 High Pass Filter (HPF)	4

I.3.3	Band-Pass Filter (BPF)	4
I.3.4	Band-Stop Filter (BSF).....	4
I.4	Methods Used in Designing Filters	4
I.4.1	Insertion loss method.....	4
I.4.1.1	Maximally flat low pass filter prototype	6
I.4.1.2	Equal ripple low pass filter prototype	7
I.4.1.3	Filter Transformation from Prototype	8
I.4.2	Image parameters method	9
I.5	Filter Design.....	10
I.5.1	Richard's Transformation.....	11
I.5.2	Kuroda's identities	12
I.5.3	Low pass filter design using stubs.....	13
I.5.4	Low pass filter design using stepped-impedances	14
I.6	Defected Ground Structure (DGS).....	16
I.6.1	DGS as periodic structures	16
I.6.2	Different forms of DGS	17
I.6.3	Equivalent circuit of DGS.....	18
I.6.4	DGS Characteristics	19
I.6.4.1	Stop-band effects	19
I.6.4.2	Slow-wave effect	19
I.6.4.3	High characteristic impedance	20
I.6.5	Advantages and Disadvantages of DGS	20
I.6.3	Advantages of DGS.....	20
I.6.4	Disadvantages of DGS.....	20

CHAPTER II: Microstrip Transmission Lines Theory

II.1	Introduction	22
II.2	History of microstrip.....	22
II.3	Microstrip transmission line.....	22
II.3.1	Definition	22
II.3.2	Application and characteristics of microstrip lines	23
II.3.3	Analysis and synthesis formulas	24
II.3.3.1	Analysis formulas.....	24
	i) Effective dielectric constant	24
	ii) Characteristic impedance	24
II.3.3.2	Analysis formulas.....	25
II.4	Guided wavelength, propagation constant, phase velocity and electrical length.....	25
II.5	Loss in microstrip	26
II.5.1	Conductor loss.....	26
II.5.2	Dielectric loss.....	26
II.5.3	Radiation loss	27
II.6	Microstrip discontinuities	27
II.6.1	Main discontinuities	27
II.6.1.1	Bend	27
II.6.1.1	Steps in width.....	28
II.6.1.2	Open ends	Erreur ! Signet non défini.
II.7	S-parameters.....	29

CHAPTER III: Design and Simulation of a novel LPF structure

III.1	Introduction.....	31
III.2	Design procedure of the proposed LPF	Erreur ! Signet non défini.
III.3	Emplementation and experimental results.....	39

III.4 Conclusion.....	42
GeneralConclusion	43
References.....	XIV
Appendix A.....	XVII
Appendix B.....	XVIII

List of Tables

Table I. 1: Element values for maximally flat low pass filter prototypes.	7
Table I. 2: Element values for equal ripple low pass filter prototypes	8
Table III. 1: Dimensions of the DGS units	31
Table III. 2: A comparison result between the filter structure without and with DGS units.....	37
Table III. 3: Simulation results.....	38
Table III. 4: Comparison of the proposed DGS-LPF with other existing LPFs	39

List of Figures

Figure I. 1: Frequency responses of the four types of filters.....	4
Figure I. 2: Two-port network with reflection coefficient.....	5
Figure I. 3: Maximally flat and equal ripple LPF (N=3).....	6
Figure I. 4: Ladder circuits for low pass filter prototypes and their element definitions.....	8
Figure I. 5: The process of filter design by the insertion loss method.....	9
Figure I. 6: Two-port network termination and its image impedances.....	9
Figure I. 7: Low pass filter sections in T and π form.....	10
Figure I. 8: Richard's transformation.....	12
Figure I. 9: The four kuroda's identities ($n^2 = 1 + Z_2/Z_1$).....	13
Figure I. 10: Equivalent circuits illustrating kurod's identity (a) in Figure I.8.....	13
Figure I. 11: Approximate equivalent circuits for short sections of transmission line.....	15
Figure I. 12: (a) A dumbbell shaped DGS etched in the ground plane of a microstrip line with periodic uniform distribution, (b) binomial distribution, (c) exponential distribution	17
Figure I. 13: Periodic DGS (a) Horizontal periodic DGS, (b) Vertical periodic DGS.....	17
Figure I. 14: Different types of DGS	18
Figure I. 15: RLC equivalent circuit for unit DGS.....	19
 Figure II. 1: View of a microstrip line and its lines of electric and magnetic fields	 23
Figure II. 2: Microstrip discontinuities bends and its equivalent circuit	27
Figure II. 3: Symmetrical microstrip steps and its equivalent circuit.....	28
Figure II. 4: Microstrip discontinuities open end	29
Figure II. 5: General two-port network S-parameters	30

Figure III. 1: The layout of the three DGS units.....	31
Figure III. 2: The simulated S-parameters of the three DGS units.....	32
Figure III. 3: Geometry of the LPF	33
Figure III. 4: S-parameters results.....	33
Figure III. 5(a): LPF using open-circuited stub.	34
Figure III. 5(b): Series-resonant branch	34
Figure III. 5(c): Series-resonantbranch loaded by radial stub	34
Figure III. 5(d): Mirrored structure.....	35
Figure III. 6: The magnitude of S21 for four steps	35
Figure III. 7: Mirrored series-resonant branch with coupled C-DGS	36
Figure III. 8: Simulation results of the proposed LPF based on Mirrored series-resonant branch along with coupled C-DGS	36
Figure III. 9: Final geometrical structure of the proposed LPF	37
Figure III. 10: S-parameters results of the proposed final LPF structure.....	38
Figure III. 11 Vector network analyzer.....	39
Figure III. 12 Photography of the fabricated of the final structure Top and Bottom view	39
Figure III. 13 Measured and simulated S11 of the final structure LPF.....	40
Figure III. 13 Measured and simulated S21 of the final structure LPF.....	41

List of Abbreviations

BPF	Band Pass Filter
RF	Radio Frequency
DGS	Defected Ground Structure
FR4	Flame Retardant 4
IEEE	Institute of Electrical and Electronic Engineers
ITT	International Telephone and Telegraph
HPF	High Pass Filter
LPF	Low Pass Filter
TEM	Transverse Electromagnetic
L_R	Return loss
TF	Transfer function
SF	Sharpness factor
IPM	Image Parameter Method
IE3D	Integral Equation Three-Dimensional (electromagnetics)
BSF	Band stop filter
EM	Electromagnetic
IL	Insertion loss
VNA	Vector Network Analyzer

List of Symbols

W	Strip line width
T	Strip line thickness
H	Substrate thickness
λ_g	Guided wavelength
β	Propagation constant
v_p	Phase velocity
θ	Electrical length
Q	Quality factor
C	Light velocity
ϵ_{eff}	Effective dielectric constant
ϵ_r	Relative Permittivity
C	Capacitance
L	Inductance
R	Resistance
Z	Impedance
Z_0	Characteristic Impedance
Y	Admittance
Y_0	Characteristic admittance
E	Electric Field
H	Magnetic Field
F	Operating frequency
f_0	Center frequency

f_c	Cutoff frequency
S_{ij}	Scattering parameters
M	Meter
S	Second
Hz	Hertz
Db	Decibel

General Introduction

Filters are playing very important roles in many RF/Microwave applications. They are commonly used to separate or combine different bands. Emerging applications such as wireless communications continue to challenge RF/Microwave filters with high performance, small size, light weight, and low cost. Depending on the requirements and specification of certain application, RF/Microwave filters may be designed as lumped element or distributed element circuits. Different classes of filters can be found in the telecommunication field, one of them is the low pass filter (LPF); they may be realized in various transmission line structures, such as waveguide, microstrip and so on [1].

At any communication system, a low pass filter is a filter that selects low frequencies up to the cutoff frequency f_c and attenuates other frequencies which are higher than f_c .

In this work, we propose a novel microstrip low pass filter with high performance (wide rejection band, low insertion loss in the pass-band, sharpness response and a compact size), will be designed using defected ground structure (DGS) technique and then, compare its characteristic performance to those reported in the literature. The numerical and EM simulations are carried out using MATLAB and Zeland IE3D software.

This report contains three chapters where the first chapter deals with the study of microwave filters, and some expressions used in filters. Then, the defected ground structure (DGS) concept. The second chapter is Overview about microstrip technology, its history, definition, applications. Then in the final chapter discusses the design of an LPF with a wide stop-band and a very low insertion loss in pass-band.

Finally, conclusion of this work and some suggestions for future works will be presented.

CHAPTER I

Literature Review of Microwave Theory

I.1 Introduction

Microwave filters are two-port network used to control the frequency response at a certain point in a microwave system by providing transmission at frequencies within the pass-band of the filter and attenuation in the stop-band of the filter. Designers needed a new procedure and structure to make low insertion loss and perfect convention simulated. Introducing Defected Ground Structure (DGS) technique is one of the key solutions to realize the superior performances [2].

In this chapter, we will discuss some filter related topics, which are the method used to design the filters, the different types of filters, some of the scientific expressions used while trying to describe a filter as well as an overview about DGS, then we will pass to the equivalent circuit and some structures based on DGS.

I.2 Expressions used in filters

I.2.1 Transfer function

Transfer function is an essential feature used in analyzing electronic systems, such as signal processing, communication systems.

In a two-port filter network, the network response characteristics are described by the transfer function different mathematical laws called filtering function, where the most ones used are: Butterworth and Chebyshev laws [3].

In RF/microwave systems, the transfer function defined by using scattering parameter S_{21} , but in general, the square of S_{21} magnitude is used instead of its magnitude only, so for a lossless passive filter network the TF is defined as [4]:

$$|S_{21}(j\omega)|^2 = \frac{1}{1 + \varepsilon^2 F_n^2(\omega)} \quad (1.1)$$

Where ω represents a frequency variable, ε is the ripple constant and $F_n(\omega)$ is the characteristic function.

I.2.2 Insertion loss

In the best possible way, an ideal filter would introduce no loss of power in the bandwidth (zero insertion loss), Actually there is a certain amount of power loss related to the filter. The insertion loss quantifies how much below the 0db line the power amplitude response drops [5].

$$IL \text{ (dB)} = -20 \log |S_{21}(j\Omega)| \quad (I.2)$$

I.2.3 Return loss

In technical terms, L_R is the ratio of the power reflected back from a device under test, by a discontinuity in a transmission line or optical fiber, to the power launched into that device, usually expressed as a negative number in dB. this discontinuity can be a mismatch with the terminating load or with a device inserted in the line. The return loss can be found by [5]:

$$L_R \text{ (dB)} = 10 \log |1 - |S_{21}(j\Omega)|^2| \quad (I.3)$$

I.2.4 Pass-band

Pass-band is the band of frequencies that is allowed to pass through a filter. Pass-band is equal to the frequency range for which the filter insertion loss is less than a specified value.

I.2.5 Cutoff frequency

Cutoff frequency is the frequency at which the filter insertion loss is equal to -3 dB.

I.2.6 Stop-band

Stop-band is equal to the frequency range at which the filter insertion loss is greater than a specified value. It is the band out of the pass band.

I.2.7 Sharpness factor

The sharpness factor is the ratio between the cutoff frequency and the resonance frequency

$$SF = \frac{f_c}{f_0} \quad \text{where } f_0 \text{ is the frequency of first pole} \quad (I.4)$$

I.3 RF/Microwave filter types

There are four primary categories of filters which are:

I.3.1 Low pass filter

A low-pass filter (LPF) is a filter that passes signals with a frequency lower than a certain cutoff frequency and attenuates (reduces the amplitude of) signals with frequencies higher than the cut-off frequency (f_c). the output at the critical frequency is 70.7% of the input. This response is equivalent to an attenuation of -3dB. The actual amount of attenuation varies from filter to other.

I.3.2 High pass filter

High-pass filter (HPF) passes all frequencies above the cutoff frequency with minimal attenuation and attenuates (reduce) signals from DC to some specified cutoff frequency. HPF are mainly used in digital image processing to perform image enhancements, edgedetection, noise reduction, [6].

In practice, due to the emergence of higher order modes, the extent of the pass band of high pass filters is limited [7].

I.3.3 Band-pass filter

A band pass filter allows signals with a range of frequencies (f_{c1} , f_{c2}). (pass band) to pass through and attenuates signals with frequencies outside this range.

I.3.4 band-reject or band stop filter

A filter with effectively the opposite function of the band-pass is the band-reject or notch filter;

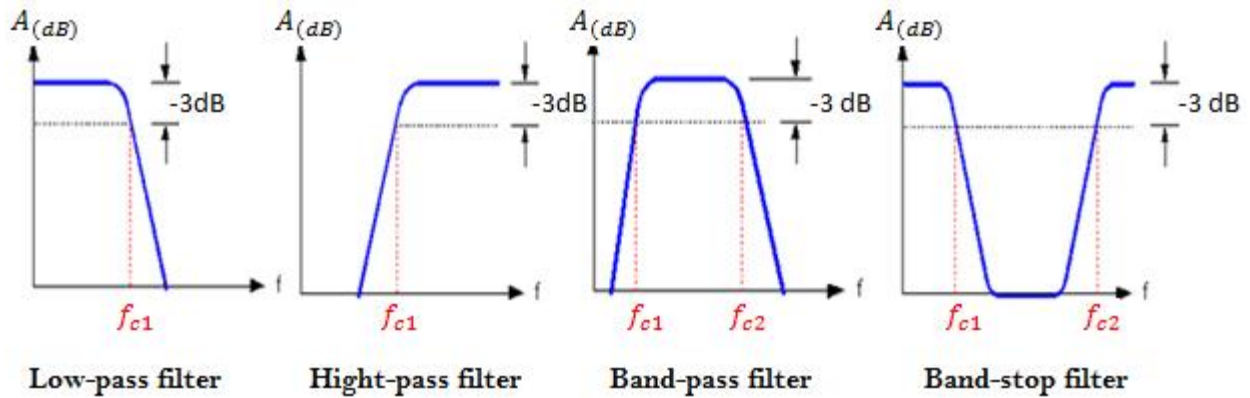


Figure.I.1. Frequency responses of the four types of filters [8].

I.4 Methods used in designing filters

I.4.1 Insertion loss method

Insertion loss method (ILM) allows a high degree of control over the stop-band amplitude and phase characteristic with a systematic way to synthesize a desired response. The necessary design trade-offs can be evaluated to the best meet of application requirements. The insertion loss method allows filter performance to be improved in straight forward manner, at the expense

of higher order filter, which is equal to the number of reactive elements. In this technique, the relative power loss due to the lossless filter with reflection coefficient $\Gamma(\omega)$ [9]

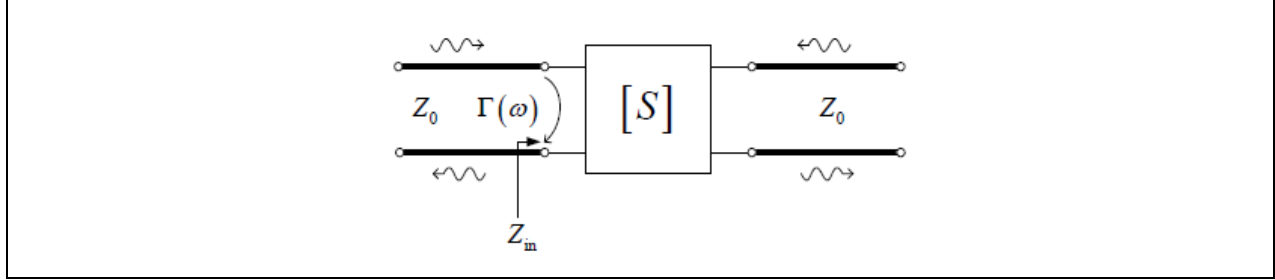


Figure I.2 Two-port network with reflection coefficient.

In the ILM a filter response is defined by its insertion loss, or power loss ratio P_{LR} .

$$P_{LR} = \frac{\text{power available from the source}}{\text{power delivered to the load}} = \frac{P_{inc}}{P_{load}} = \frac{P_0}{P_0[1-|\Gamma(\omega)|^2]} = \frac{1}{1-|\Gamma(\omega)|^2} \quad (I.5)$$

Note from this definition $P_{LR} = \infty$ when $\Gamma(\omega) = 1$ and $P_{LR} = 1$ when $\Gamma(\omega) = 0$.

If both the source and load ports are matched for this network, then $P_{LR} = |S_{21}|^2$. The insertion loss (IL) in dB:

$$IL = 10 \log |S_{21}|^2 \quad (I.6)$$

The power loss ratio in dB is simply the insertion loss of a filter, thus filter design using the power loss ratio is also called the insertion loss method, and since $|\Gamma(\omega)|^2$ is an even function of ω , so it can be expanded in a polynomial series in ω^2 . In particular, for a linear and time invariant system, $|\Gamma(\omega)|^2$ is a rational function

$$|\Gamma(\omega)|^2 = \left| \frac{Z_{in}(\omega) - Z_0}{Z_{in}(\omega) + Z_0} \right|^2 \quad (I.7)$$

This means that it can be expressed as quotient of polynomial (real and nonnegative) $M(\omega^2)$ and $N(\omega^2)$ Where M and N are real polynomial in ω^2 .

$$|\Gamma(\omega)|^2 = \frac{M(\omega^2)}{M(\omega^2) + N(\omega^2)} \quad (I.8)$$

Substituting the above relation in P_{LR} relation we obtain the following:

$$P_{LR} = 1 + \frac{M(\omega^2)}{N(\omega^2)} \quad (I.9)$$

Thus, a filter to be physically realizable its power must be of the form of the above equation. Notice that specifying the power loss ratio simultaneously constrains the reflection coefficient.

I.4.1.1 Maximally flat low pass filter prototype

This characteristic is also called the binomial or Butterworth response, and it is optimum in the sense that it provides the flattest pass-band response for a given filter complexity or order. For low pass filter it is specified by: [9]

$$P_{LR} = 1 + k^2 \left(\frac{\omega}{\omega_c} \right)^{2N} \quad (I.10)$$

where N is the order of the filter, and ω_c is the cutoff frequency. The pass-band extends from $\omega = 0$ to $\omega = \omega_c$ at the band edge the power loss ratio is $1+k^2$.

For $\omega > \omega_c$, the attenuation increases monotonically with frequency as in the Figure I.3. For

$$\omega \gg \omega_c: \quad P_{LR} \cong k^2 \left(\omega / \omega_c \right)^2 \quad (I.11)$$

This shows that the insertion loss increases at rate of $20N$ dB/decade.

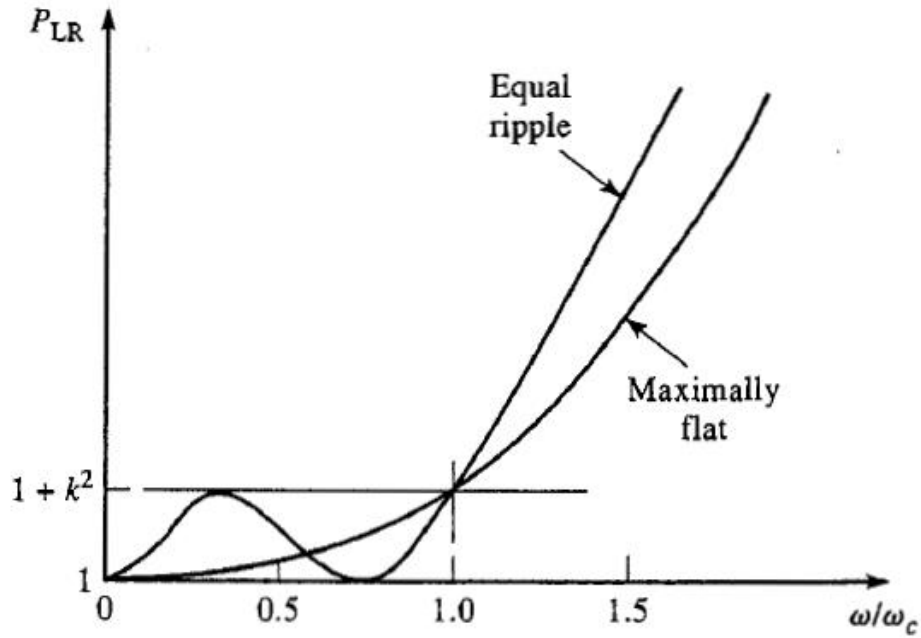


Figure I.3 Maximally flat and equal ripple LPF (N=3).

Table I.1 Element values for maximally flat low pass filter prototypes ($g_0 = 1, \omega_c = 1, N = 1$ to 10) [10].

N	g_1	g_2	g_3	g_4	g_5	g_6	g_7	g_8	g_9	g_{10}	g_{11}
1	2.0000	1.0000									
2	1.4142	1.4142	1.0000								
3	1.0000	2.0000	1.0000	1.0000							
4	0.7654	1.8478	1.8478	0.7654	1.0000						
5	0.6180	1.6180	2.0000	1.6180	0.6180	1.0000					
6	0.5176	1.4142	1.9318	1.9318	1.4142	0.5176	1.0000				
7	0.4450	1.2470	1.8019	2.0000	1.8019	1.2470	0.4450	1.0000			
8	0.3902	1.1111	1.6629	1.9615	1.9615	1.6629	1.1111	0.3902	1.0000		
9	0.3473	1.0000	1.5321	1.8794	2.0000	1.8794	1.5321	1.0000	0.3473	1.0000	
10	0.3129	0.9080	1.4142	1.7820	1.9754	1.9754	1.7820	1.4142	0.9080	0.3129	1.0000

Source: Reprinted from G. L. Matthaei, L. Young, and E. M. T. Jones, *Microwave Filters, Impedance-Matching Networks, and Coupling Structures* (Dedham, Mass.: Artech House, 1980) with permission.

I.4.1.2 Equal ripple low pass filter prototype

If the Chebyshev polynomial is used to specify the insertion loss of an N-order low pass filter,

$$P_{LR} = 1 + k^2 T_N^2\left(\frac{\omega}{\omega_c}\right) \quad (I.12)$$

A sharper cutoff will result; although the pass-band response will have ripples of amplitude $1+k^2$ as shown in Figure I.3. Since $T_N(x)$ oscillates between ± 1 for $|x| \leq 1$ thus k^2 determines the pass-band ripple level. For large x , $T_N(x) \cong \frac{1}{2}(2x)^N$, so for $\omega \gg \omega_c$ the insertion loss becomes:

$$P_{LR} \cong \frac{k^2}{4} \left(\frac{2\omega}{\omega_c}\right)^{2N} \quad (I.13)$$

Table I.2 Element values for equal ripple low pass filter prototypes ($g_0 = 1, \omega_c = 1, N = 1$ to 10) [10].

N	0.5 dB Ripple										
	g_1	g_2	g_3	g_4	g_5	g_6	g_7	g_8	g_9	g_{10}	g_{11}
1	0.6986	1.0000									
2	1.4029	0.7071	1.9841								
3	1.5963	1.0967	1.5963	1.0000							
4	1.6703	1.1926	2.3661	0.8419	1.9841						
5	1.7058	1.2296	2.5408	1.2296	1.7058	1.0000					
6	1.7254	1.2479	2.6064	1.3137	2.4758	0.8696	1.9841				
7	1.7372	1.2583	2.6381	1.3444	2.6381	1.2583	1.7372	1.0000			
8	1.7451	1.2647	2.6564	1.3590	2.6964	1.3389	2.5093	0.8796	1.9841		
9	1.7504	1.2690	2.6678	1.3673	2.7239	1.3673	2.6678	1.2690	1.7504	1.0000	
10	1.7543	1.2721	2.6754	1.3725	2.7392	1.3806	2.7231	1.3485	2.5239	0.8842	1.9841

After selecting the appropriate low pass filter prototype that meets the given specifications, the following circuits are used to design the LPF.

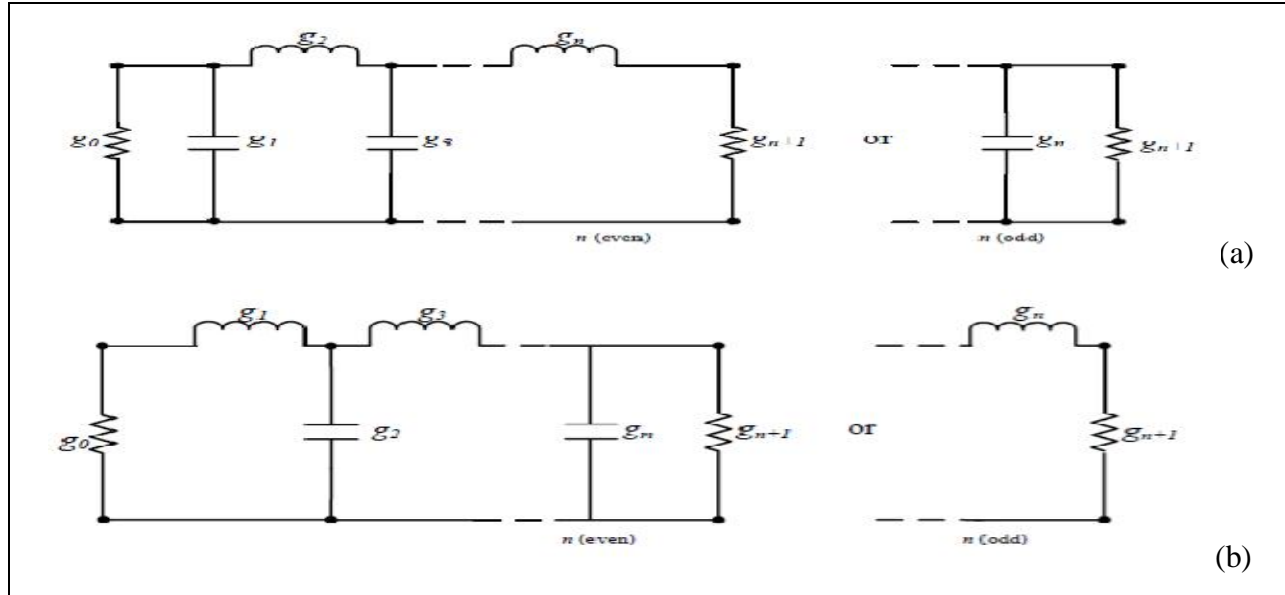


Figure I.4 Ladder circuits for low pass filter prototypes and their element definitions.

(a) Prototype beginning with a shunt element. (b) Prototype beginning with a series element.

I.4.1.3 Filter transformation from prototype

In order to design actual low pass, high pass, band-pass and band-stop filters, the transformations of low pass prototype filters with normalized cutoff frequency $\omega_c=1$ and having the source and load resistances of $R_s=1\Omega$ are made into the desired type with required source and load impedances using frequency and impedance transformations.

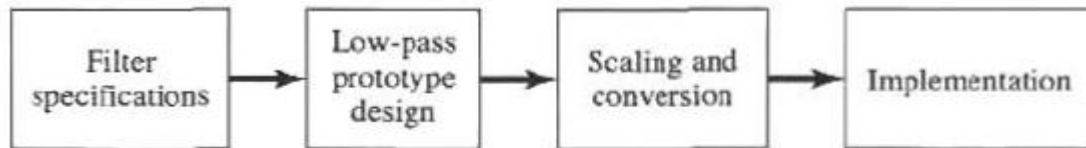


Figure I.5 The process of filter design by the insertion loss method.

I.4.2 Image parameters method

The image parameter method (IPM) is useful in studying filters and solid-state traveling wave amplifier design. Consider the following two-port network shown in Figure I.6 Z_{i1} and Z_{i2} are called image impedances. Both ports are matched when terminated in their image impedances.

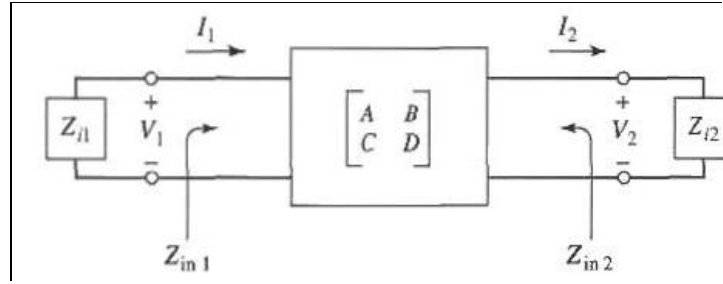


Figure I.6 Two-port network termination and its image impedances.

It can be proved mathematically, using ABCD matrix and calculating Z_{i1} and Z_{i2}

$$Z_{i1} = \sqrt{\frac{AB}{CD}} \quad (I.14)$$

$$Z_{i2} = \sqrt{\frac{BD}{AC}} \quad (I.15)$$

In addition, the propagation factor of the network is given as

$$\cosh \gamma = \sqrt{AD} \quad (I.16)$$

$$\gamma = \alpha + j\beta \quad (I.17)$$

The above result used in the analysis of coupled line filter.

The following figure shows how to construct an LPF circuit with IPM with these lumped elements.

$$L = 2R_0/\omega_c C = 2/\omega_c R_0 \quad (I.18)$$

$$R_0 = \sqrt{L/C}\omega_c = 2\pi/\sqrt{LC} \quad (I.19)$$

ω_c : is the cutoff frequency; R_0 : is the nominal characteristic impedance

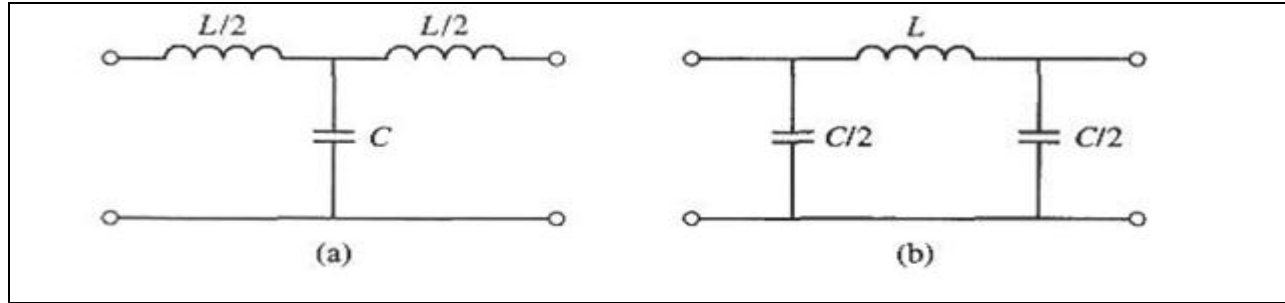


Figure I.7 Low pass filter sections in T and π form
(a) T-section. (b) π -section.

I.5 Filter design

The lumped-element filter design discussed in the previous sections generally works well at low frequencies, but two problems arise at microwave frequencies. First, lumped elements such as inductors and capacitors are generally available only for a limited range of values and are difficult to implement at microwave frequencies, but must be approximated with distributed components. In addition, at microwave frequencies the distances between filter components is not negligible. Richard's transformation is used to convert lumped elements to transmission line sections, while Kuroda's identities can be used to separate filter elements by using transmission line sections. Because such additional transmission line sections do not affect the filter response, this type of design is called redundant filter synthesis. It is possible to design microwave filters that take advantage of these sections to improve the filter response [11]; such nonredundant synthesis does not have a lumped-element counterpart.

I.5.1 Richard's Transformation

The transformation, given by expression (I.20), maps the ω plane to the Ω plane, which repeats with a period of $\frac{\omega \ell}{v_p} = 2\pi$. This transformation was introduced by P. Richard [12] to synthesize an LC network using open- and short-circuited transmission lines.

$$\Omega = \tan(\beta \ell) = \tan\left(\frac{\omega \ell}{v_p}\right) \quad (\text{I.20})$$

If we replace the frequency variable ω with Ω , the reactance of an inductor can be written as

$$jX_L = j \Omega L = jL \tan(\beta\ell) \quad (I.21)$$

and the susceptance of a capacitor can be written as

$$jB_C = j \Omega C = jC \tan(\beta\ell) \quad (I.22)$$

These results indicate that an inductor can be replaced with a short-circuited stub of length $\beta\ell$ and characteristic impedance L , while a capacitor can be replaced with an open-circuited stub of length $\beta\ell$ and characteristic impedance $\frac{1}{C}$. A unity filter impedance is assumed.

Cutoff occurs at unity frequency for a low pass filter prototype; to obtain the same cutoff frequency for the Richard's transformed filter, (I.20) shows that

$$\Omega = 1 = \tan(\beta\ell) \quad (I.23)$$

which gives a stub length of $\ell = \lambda/8$, where λ is the wavelength of the line at the cutoff frequency, ω_c . At the frequency $\omega_0 = 2\omega_c$, the lines will be $\lambda/4$ long and an attenuation pole will occur. At frequencies away from ω_c , the impedances of the stubs will no longer match the original lumped-element impedances, and the filter response will differ from the desired prototype response. Also, the response will be periodic in frequency, repeating every $4\omega_c$.

In principle, then, the inductors and capacitors of a lumped-element filter design can be replaced with short-circuited and open-circuited stubs, as illustrated in Figure I.8. Since the lengths of all the stubs are the same ($\lambda/8$ at ω_c), these lines are called commensurate lines.

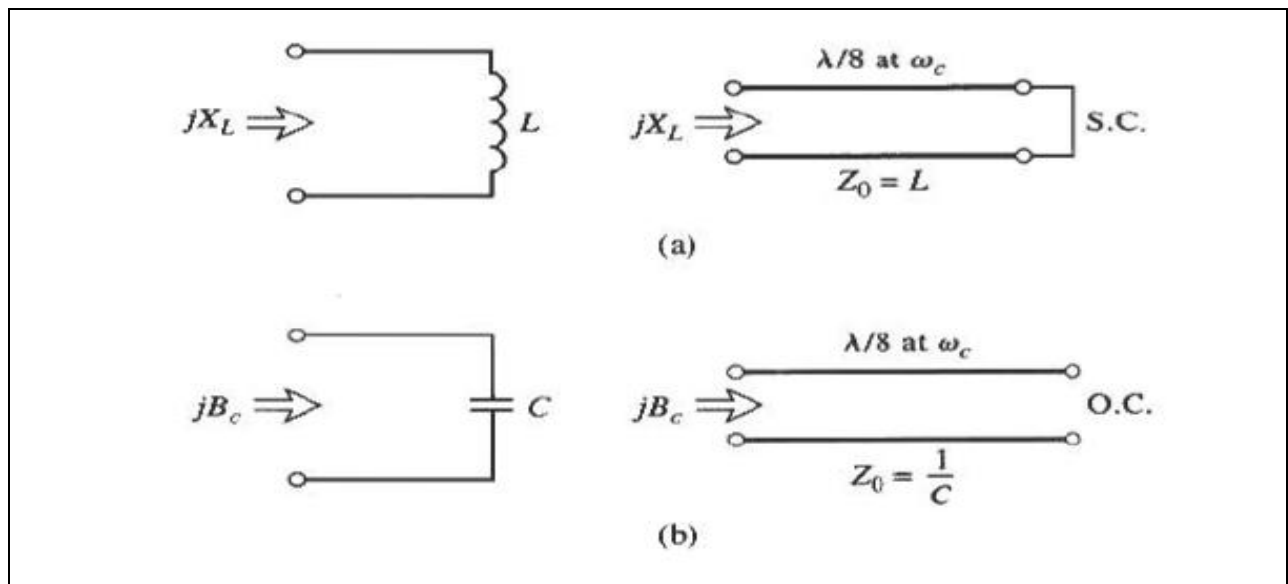


Figure I.8 Richard's transformation. (a) For an inductor to a short-circuited stub.
(b) For a capacitor to an open-circuited stub.

I.5.2 Kuroda's identities

The four Kuroda's identities use redundant transmission line sections to achieve a more practical microwave filter implementation by performing any of the following operations

- Physically separate transmission line stubs;
- Transform series stubs into shunt stubs, or vice versa and
- Change impractical characteristic impedances into more realizable ones.

The additional transmission line sections are called unit elements and are $\lambda/8$ long at ω_C ; the unit elements are those commensurate with the stubs used to implement the inductors and capacitors of the prototype design.

The four identities are illustrated in Figure I.9, where each box represents a unit element, or transmission line of the indicated characteristic impedance and length ($\lambda/8$ at ω_C). The inductors and capacitors represent short-circuit and open-circuit stubs, respectively.

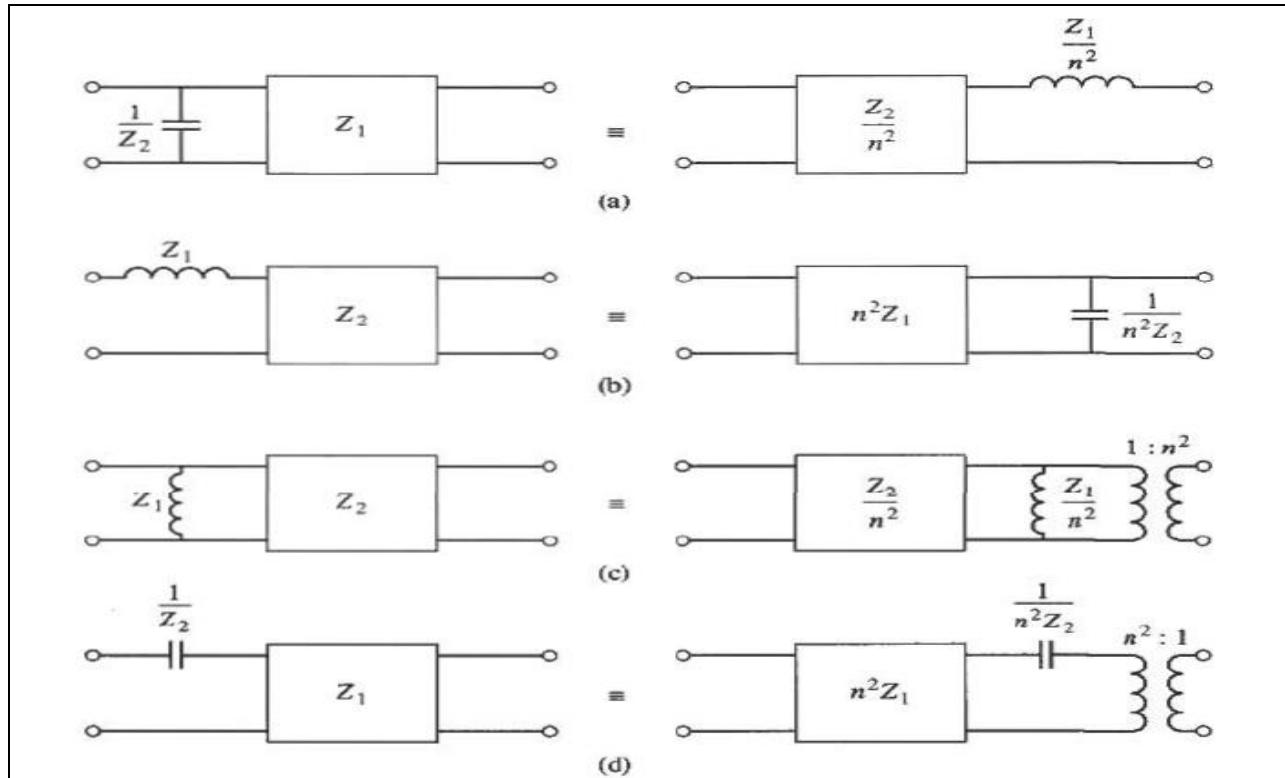


Figure I.9 The four Kuroda's identities ($n^2 = 1 + Z_2/Z_1$)

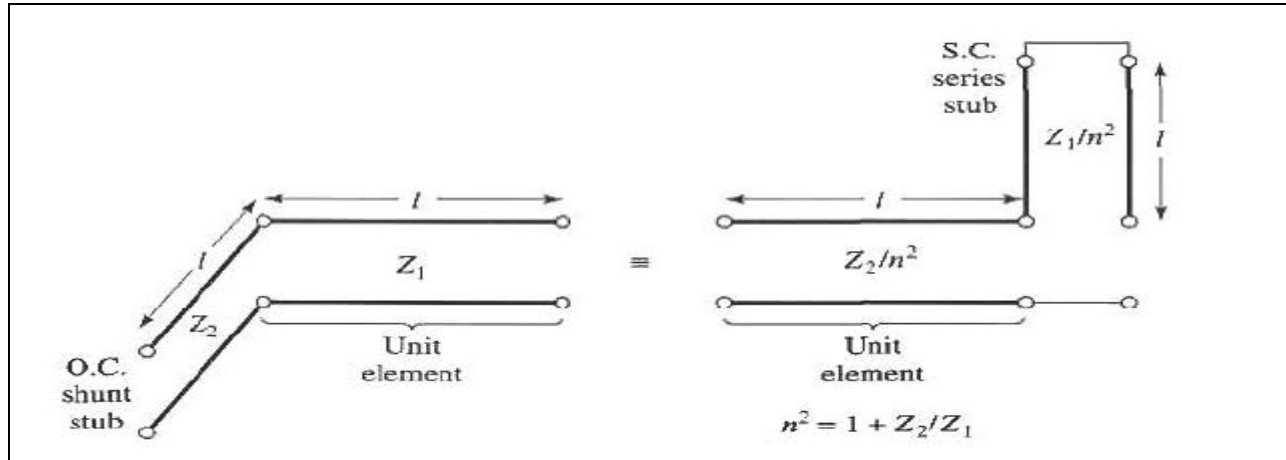


Figure I.10Equivalent circuits illustrating Kuroda's identity (a) in Figure I.8.

I.5.3 Low pass filter design using stubs

First, the design of the lumped element circuit with the required response is performed using the insertion loss method (maximally flat or equal ripple for example). The next step is to use Richard's transformation to convert series inductors to series stubs, and shunt capacitors to shunt stubs. The characteristic impedance of a series stub (inductor) is L , and the characteristic impedance of a shunt stub (capacitor) is $\frac{1}{C}$. For commensurate line synthesis, all stubs are $\lambda/8$ long at $\omega = \omega_c$ (cutoff frequency). It is more convenient to work with normalized quantities until the last step in the design. Because series stubs would be very difficult to implement in practice, one of the Kuroda's identities is used to convert these to shunt stubs. In order to do this, unit elements ($\lambda/8$ long at ω_c) are added at either end of the filter. These redundant elements do not affect filter performance since they are matched to the source and load. Then we can apply Kuroda's identity to both ends of filter. Finally, the circuit is implemented and frequency scaled. By doing that, the desired response is obtained in the pass-band of the filter, but it will be repeated periodically because of the nature of Richard's transformation.

I.5.4 Low pass filter design using stepped-impedances

An easy way to implement low pass filters in microstrip or strip lines is to use alternating sections of very high and very low characteristic impedance lines. Such filters may be called High-Z or Low-Z filters. The advantages over shunt-stub filters are that they are easier to fabricate and take up less space. One disadvantage is that this method uses approximations that

will lead to an electrical performance that is not very good; this type doesn't give a sharp cutoff. This must be considered when a filter is required in a certain application. It can be shown that the Z-parameters of a length ℓ of line having characteristic impedance Z_0 are given by: [9]

$$Z_{11} = Z_{22} = \frac{A}{C} = -jZ_0 \cot \beta \ell \quad (I.24)$$

$$Z_{12} = Z_{21} = \frac{1}{C} = -jZ_0 \csc \beta \ell \quad (I.25)$$

The series elements of the T-equivalent circuit are [4]

$$Z_{11} - Z_{22} = -j Z_0 \left[\frac{\csc \beta \ell - 1}{\sin \beta \ell} \right] = jZ_0 \tan \frac{\beta \ell}{2} \quad (I.26)$$

While the shunt element of the T-equivalent is Z_{12} . So, if $\beta \ell < \pi/2$, the series elements have a positive reactance (inductors), while the shunt element has a negative reactance (capacitor). We thus have the equivalent circuit shown in Figure I.11 (a), where

$$\frac{X}{2} = Z_0 \tan \frac{\beta \ell}{2} \quad (I.27)$$

$$B = \frac{1}{Z_0} \sin \beta \ell \quad (I.28)$$

Now assume a short length of line ($\beta \ell < \pi/4$) and a large characteristic impedance. Then, the above relations are reduced to

$$X \approx Z_0 \beta \ell \quad (I.29)$$

$$B \approx 0 \quad (I.30)$$

This gives the series inductor

Now, for a short length of line and small characteristic impedance

$$X \approx 0 \quad (I.31)$$

$$B \approx Y_0 \beta \ell \quad (I.32)$$

This implies a shunt capacitor.

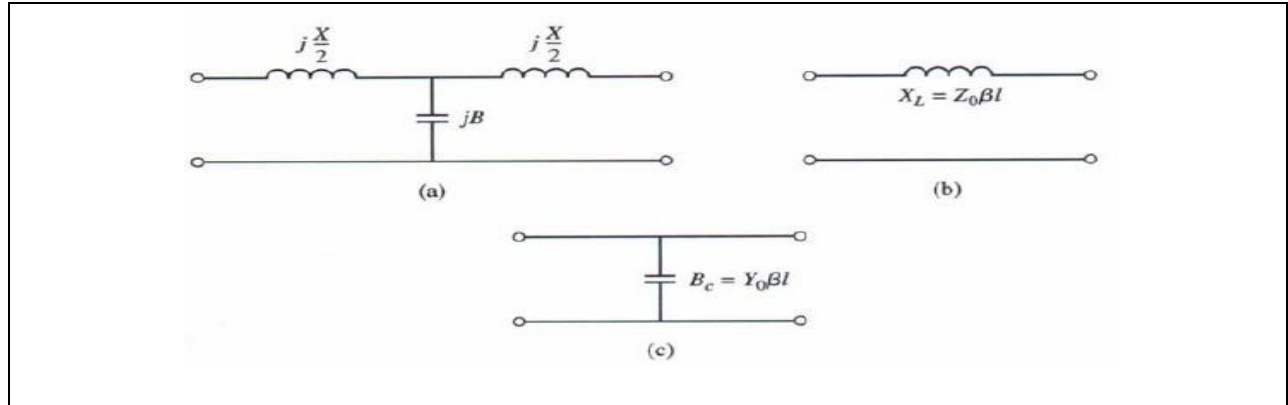


Figure I.11 Approximate equivalent circuits for short sections of transmission line.

So, the series inductors of a low pass prototype can be replaced with a high impedance line sections ($Z_0=Z_h$), and the shunt capacitors can be replaced with low impedance line sections ($Z_0=Z_\ell$). The ratio $\frac{Z_h}{Z_\ell}$ should be as high as possible, so the actual values of Z_h and Z_ℓ are usually set to be the highest and the lowest characteristic impedances that can be practically fabricated. The lengths of the lines are evaluated at the cutoff frequency, and can be calculated as follows:

The electrical length of the inductor section is

$$\beta\ell = \frac{LR_0}{Z_h} \quad (I.33)$$

And the electrical length of capacitor section is

$$\beta\ell = \frac{CZ_\ell}{R_0} \quad (I.34)$$

Where R_0 is the filter impedance, L and C are the normalized element values of the low pass prototype [4].

I.6 Defected Ground structures (DGS)

Over the past few years, there has been a different new concept applied in order to distribute microwave circuits. The one of these techniques is defected ground structure or DGS, where the ground plane metal of a microstrips circuit is intentionally modified to enhance performances. This technique's name simply means that a "defect" has been placed in the ground plane, what is generally regarded as an approximation of 'an infinite, current collector perfectly-conducting. Indeed, a ground plane at microwave frequencies is far removed from the idealized behavior of

perfect ground. Although the additional perturbations of DGS alter the uniformity of the ground plane, they do not render it defective [13].

I.6.1 DGS as Periodic Structures

Since last few years, almost 2001, many searchers have been tried to use periodic DGSs to improve the performance of amplifiers, power dividers, and oscillators, so they suggested to use a micro strip line with periodic DGS at the output for harmonic tuning of different components. A periodic uniform dumbbell shaped DGS is used in order to suppress the higher order modes of a power amplifier. Later on, 2004 they commenced considering the non-uniform periodic DGS with relative amplitude distribution following a chebyshev or binomial distribution or exponential function, as shown in Figure I.12.

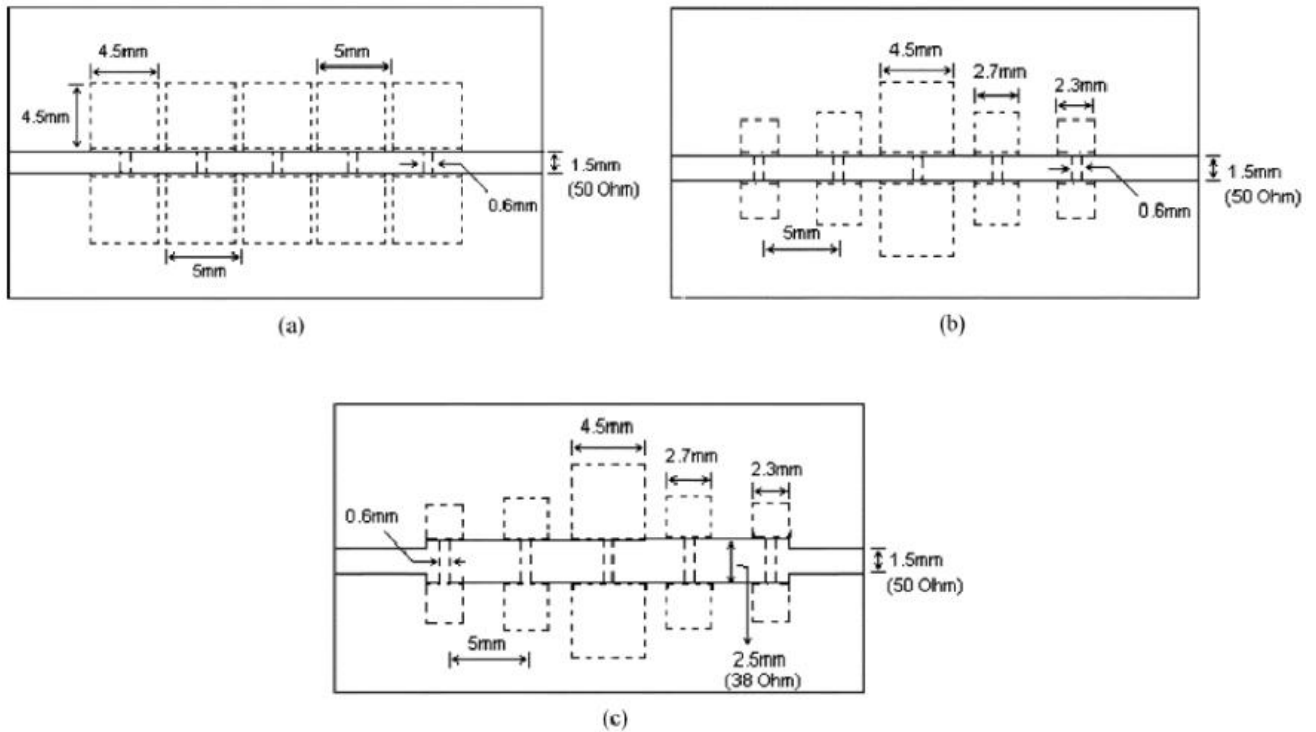


Figure I.12. (a) A dumbbell shaped DGS etched in the ground plane of a microstrip line with periodic uniform distribution, (b) binomial distribution, (c) exponential distribution [14].

Other types of P-DGS are represented in Figure.I.13

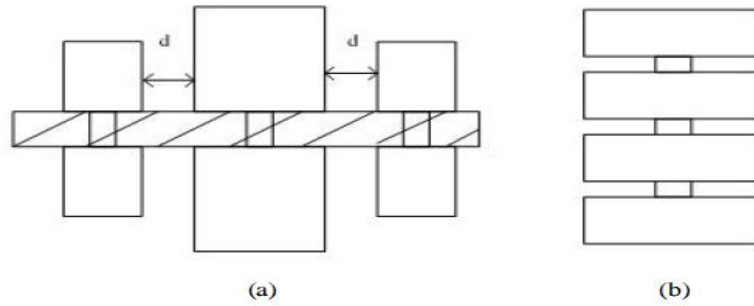


Figure I.13 Periodic DGS (a) Horizontal periodic DGS, (b) Vertical periodic DGS.

I.6.2 Different forms of DGS

Many various shapes of DGS have been studied such as a concentric ring circle, spiral, dumbbells, elliptical and U- and V- slots. Each DGS form can be represented as a circuit consisting of inductance and capacitance, which can lead to a certain frequency band gap determined by the shape, dimension and position of the defect.

DGS furnish a supplementary degree of liberty in microwave circuit design and can be used for different types of utilization [15].

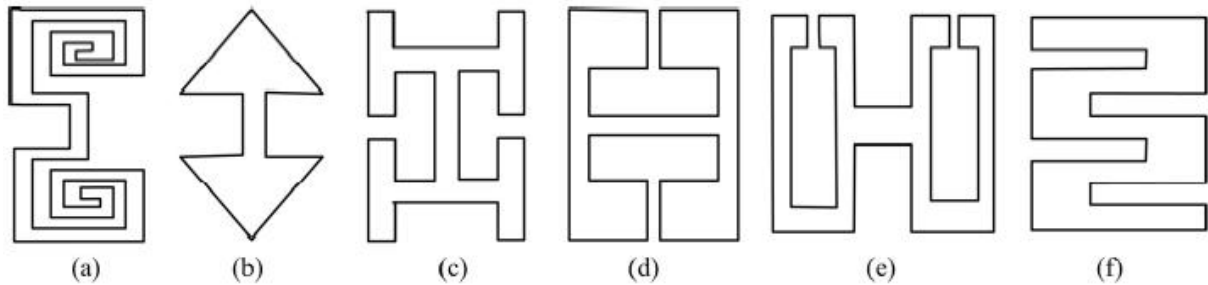


Figure I.14. Different types of DGS: (a) spiral head (b) arrow-head slot (c) “H” shape slot (d) square open-loop with a slot in middle section (e) open loop dumbbell

(f) interdigital DGS [20].

I.6.3 Equivalent circuit of DGS

Design and analysis are two challenges for DGS. The commercially available EM solvers are the main resource to design and analyze DGS. To apply the proposed DGS section to a practical

circuit design example, it is necessary to extract the equivalent circuit parameters. In order to derive the equivalent circuit parameters of DGS unit at the reference plane, the S-parameters vs. frequency should be calculated by full-wave electromagnetic (EM) simulation to explain the cutoff and attenuation pole characteristics of the DGS section. The circuit parameters for the derived equivalent circuit can be extracted from the simulation result which can be fit for the one-pole Butterworth type low pass response. The full-wave analysis does not give any physical insight of the operating principle of DGS.

DGS unit can be modeled most efficiently by a parallel R, L, and C resonant circuit connected to transmission lines at its both sides as shown in the Figure I.15. This resistance corresponds to the radiation, conductor and dielectric losses in the defect. From EM simulations or measurements for a given DGS, the equivalent R, L, and C values are obtained from the expression in [16].

$$C = \frac{\omega_c}{2Z_0(\omega_0^2 - \omega_c^2)} \quad (I.35)$$

$$L = \frac{1}{\omega_0^2 C} \quad (I.36)$$

$$R = \frac{2Z_0}{\sqrt{\frac{1}{|s_{11}(\omega_0)|^2} - \left(2Z_0\left(\omega_0 C - \frac{1}{\omega_0 L}\right)\right)^2 - 1}} \quad (I.37)$$

where $\omega_0 (=2\pi f_0)$ and $\omega_c (=2\pi f_c)$ are respectively the angular resonant frequency and 3-dB cutoff frequency. The following figure shows the DGS unit equivalent circuit.

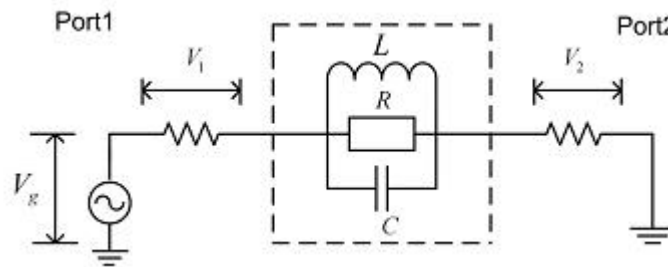


Figure I.15 RLC equivalent circuit for unit DGS.

I.6.4 DGS Characteristics

DGS has three main characteristics: Stop-band characteristics in microwave circuits, slow-wave propagation in pass-band, and high characteristic impedance [17].

I.6.4.1 Stop-band effects

DGS, which is realized by etching off a defected pattern or periodic structures from the backside metallic ground plane, has been known as providing rejection of certain frequency band, namely, bandgap effects. The stop-band is useful to suppress the unwanted surface waves, spurious and leakage transmission. Therefore, a direct application of such frequency selective characteristics in microwave filters is becoming a hotspot research recently.

Several improvements are obtained using DGS. These improvements are summarized as follows:

- More transition sharpness;
- Suppressing higher harmonic;
- Achieve broader stop-band responses and
- Improving the stop-band and pass-band characteristics.

I.6.4.2 Slow-wave effect

This is the one of the most important characteristics of DGS that the slow-wave effect which caused by the equivalent LC circuit component. The DGS is considered as an equivalent circuit consisting of capacitance and inductance as shown in Figure I.15, the equivalent inductive part increases due to the defect and produces equivalently a high effective dielectric constant that is slow-wave property. Due to this fact the DGS line has a longer electrical length than the standard microstrip line for the same physical length. Compared to a microstrip line without a DGS unit, the microstrip line with the DGS unit exhibits a faster phase variation, which exhibits slow-wave behaviors below ω_0 and a slower phase variation which exhibits fast wave behaviors beyond ω_0 , ($\omega_0 = 2\pi f_0$).

when $\omega < \omega_0$, $\omega_0 L < \frac{1}{\omega_0 C}$, inductive microstrip is achieved and when $\omega > \omega_0$ (frequencies greater than the resonance frequency of defect)

$\omega_0 L > \frac{1}{\omega_0 C}$, capacitive microstrip line is obtained and in the case at the resonance frequency

($\omega = \omega_0$ and $\omega_0 L = \frac{1}{\omega_0 C}$) a jumping phenomenon occurs [18].

I.6.4.3 High characteristic impedance

In conventional microstrip line, the generally accepted impedance is limited to $\sim 100 - 130\Omega$. By adopting the DGS on the ground plane, the effective inductance will decrease at the same time, and finally the impedance of the transmission increases to more than 200Ω [17].

I.6.5 Advantages and disadvantages of DGS

I.6.5.1 advantage of DGS

The most important characteristics of DGS are:

- ✓ Disturbs shielding fields on the ground plane;
- ✓ Increases effective permittivity;
- ✓ One-pole LPF characteristics;

I.6.5.2 Disadvantages of DGS

The DGS have a principal disadvantage which is radiations. Radiation within enclosed microwave circuits can be difficult to include in simulation. Limit conditions are usually set to be absorbing (no reflections), which make simpler calculations, but eliminate the structures around the circuit being tested.

In some cases, the size of the enclosure will make the problem too large to achieve a solution in a reasonable time, and the details of the physical structure may take a very long to determine and enter into the software [19].

Also, the EM simulation is assuredly accurate for the circuit itself, but with uncertainty of radiation effects, the construction and careful evaluation of a prototype is strongly recommended. An experienced designer may be able to create a simplified model of the enclosure for more accurate simulation, but measurement remains essential for verification. A lesser disadvantage is that DGS structures increase the area of the circuit. However, the additional area will usually be less than that of alternative solutions for achieving similarly improved performance [20].

CHAPTER 11

Microstrip Transmission Lines Theory

II.1 Introduction

Microstrip lines are very important components in the design of any printed filter. For microwave device applications, microstrip filters generally offer the smallest sizes and the easiest fabrication. Microstrip lines can be designed for frequencies that are ranging from a few Gigahertz, or even lower, up to at least many tens of Gigahertz [21].

This chapter contains the following sections: firstly, we will highlight some outlines about microstrip line history, definition, applications and characteristics, in addition to some analysis and synthesis formulas. Next, an overview about the loss in microstrip and microstrip discontinuities, finally, an overview about scattering parameters will be reported where we will emphasis on dispersion matrix of two port network.

II.2 History of microstrip

Microstrip is a planar transmission line which was developed by ITT laboratories as a competitor to stripline (first published by Grieg and Engelmann in the December 1952 IRE proceedings). According to Pozar [10], early microstrip work used fact substrates, which allowed non-TEM waves to propagate which makes results unpredictable. In the 1960s the version of microstrip became popular.

II.3 Microstrip transmission line

II.3.1 Definition

Microstrip transmission line is the most popular and used planar transmission line in radio frequency RF applications, exploited for designing certain components like filters, coupler and transformers. The wave type propagating in this transmission line is a quasi-transversal electromagnetic wave quasi-TEM. The microstrip transmission line consists of metallic strip of width “ W ” and thickness “ t ”, metallic ground and between its dielectric substrate with constant of thickness “ h ” [21], as shown in Figure II.1 The characteristic impedance of the line is determined in terms of width W , thickness t and dielectrics substrate.

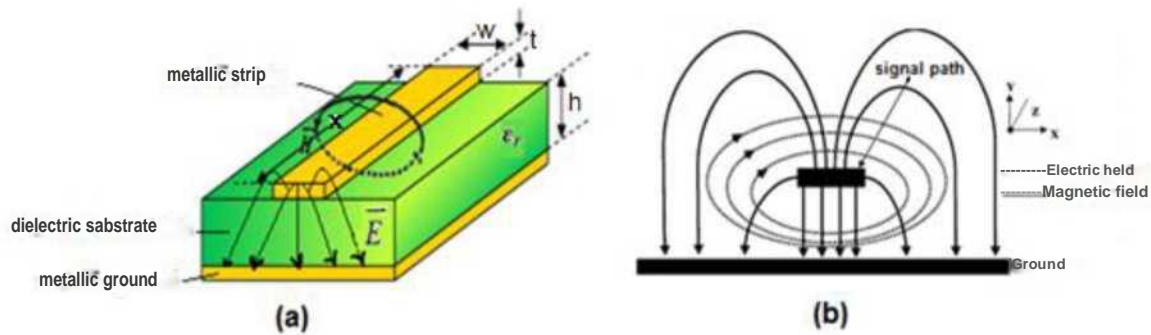


Figure.II.1. View of a microstrip line and its lines of electric and magnetic fields, (a) whole view, (b) zoom in [13,20].

- Both electric and magnetic fields are present in the transmission lines. These fields are perpendicular to each other and to direction of wave propagation for TEM mode wave, which is the simplest mode, and assumed for most simulators (except for microstrip lines which assume quasi-TEM, which is an approximated equivalent for transient response calculations).
- Electric field is established by a potential difference between two conductors: implies equivalent circuit model must contain capacitor.
- Magnetic field induced by current flowing on the line: implies equivalent circuit model must contain inductor

II.3.2 Application and characteristics of microstrip lines

Microstrip lines can be used in the manufacturing of some microwave components, therefore Low pass filters can be made from them. Due to some suitable features, microstrip line is widely used (regardless of low power handling capacity) in the transmission of microwave frequency signals. The features may include [22]:

- ✓ Its simple geometry;
- ✓ Small size and low cost;
- ✓ Absence of difficulties in devices integration and mass production;
- ✓ Good repeatability and reproducibility.

II.3.3 Analysis and synthesis formulas

II.3.3.1 Analysis formulas

Analysis formulas are used to find Z_0 and ϵ_{eff} when $\left(\frac{W}{h}\right)$ and ϵ_r are given. In these calculations, the strip thickness is neglected because its effects are usually small [23].

i) Effective dielectric constant

The effective dielectric constant is given by:

- When $\left(\frac{W}{h}\right) < 1$

$$\epsilon_{eff} = \frac{\epsilon_r + 1}{2} + \frac{\epsilon_r - 1}{2} \left[\left(1 + 12 \frac{h}{W}\right)^{-\frac{1}{2}} + 0.04 \left(1 - \frac{W}{h}\right)^2 \right] \quad (II. 1)$$

- When $\left(\frac{W}{h}\right) \geq 1$

$$\epsilon_{eff} = \frac{\epsilon_r + 1}{2} + \frac{\epsilon_r - 1}{2} \left(1 + 12 \frac{h}{W}\right)^{-\frac{1}{2}} \quad (II. 2)$$

Note that there are two implications in these equations:

First, the effective dielectric constant is involved here because some of the electric field passes directly from the bottom of the strip width to the ground plane whereas some of the electric field travels via air and the substrate to the ground plate. Second, there are two approximations for the effective dielectric constant as a function of the ratio of the width to the height, when $\left(\frac{W}{h}\right) < 1$ and when $\left(\frac{W}{h}\right) \geq 1$.

ii) Characteristic impedance

The characteristic impedance Z_0 is also calculated using separate solutions depending on the ratio of the width to the height.

- When $\left(\frac{W}{h}\right) < 1$

$$Z_0 = 60 * (\epsilon_{eff})^{-\frac{1}{2}} * \ln \left(\frac{8h}{W} + 0.25 \frac{W}{h} \right) (Ohms) \quad (II. 3)$$

- When $\left(\frac{W}{h}\right) \geq 1$

$$Z_0 = \frac{120\pi(\epsilon_{eff})^{-\frac{1}{2}}}{\frac{W}{h} + 1.393 + 0.667 \ln\left(\frac{W}{h} + 1.444\right)} (Ohms) \quad (II.4)$$

II.3.3.2 Synthesis formulas

Synthesis formulas are available for finding $\left(\frac{W}{h}\right)$ and ϵ_{eff} when Z_0 and ϵ_r are known [10].

For a narrow strip :

$$\frac{w}{h} = \left(\frac{\exp H'}{8} - \frac{1}{4 \exp H'} \right)^{-1} \quad (II.5)$$

where

$$H' = \frac{Z_0 \sqrt{2(\epsilon_r + 1)}}{119.9} + \frac{1}{2} \left(\frac{\epsilon_r - 1}{\epsilon_r + 1} \right) \left(\ln \frac{\pi}{2} + \frac{1}{\epsilon_r} \ln \frac{4}{\pi} \right) \quad (II.6)$$

And, for a wide strip :

$$\frac{w}{h} = \frac{2}{\pi} [(d_\epsilon - 1) - \ln(2d_\epsilon - 1)] + \frac{\epsilon_r - 1}{\pi \epsilon_r} [\ln(d_\epsilon - 1) + 0.293 - 0.517/\epsilon_r] \quad (II.7)$$

where

$$d_\epsilon = \frac{59.95\pi^2}{Z_0 \sqrt{\epsilon_r}} \quad (II.8)$$

$$\epsilon_{eff} = \frac{\epsilon_r + 1}{2} + \frac{\epsilon_r - 1}{2} \left(1 + \frac{10h}{W} \right)^{-0.555} \quad (II.9)$$

Alternatively, where Z_0 is known at first:

$$\epsilon_{eff} = \frac{\epsilon_r}{0.96 + \epsilon_r(0.109 - 0.004\epsilon_r)[\log(10 + Z_0) - 1]} \quad (II.10)$$

II.4 Guided wavelengths, propagation constant, phase velocity and electrical length

the guided wavelength of the quasi-TEM mode of microstrip is given by (for non-magnetic material) [24]:

$$\lambda_g = \frac{\lambda_0}{\sqrt{\epsilon_{eff}}} \quad (II.11)$$

where λ_0 is the free space wavelength at operation frequency f .

More conveniently, where the frequency is given in gigahertz (GHz), the guided wavelength can be evaluated directly in millimeters as follows [25]:

$$\lambda_g = \frac{3 \times 10^8}{f_{\text{(GHz)}} \sqrt{\epsilon_{\text{eff}}}} \text{ mm} \quad (\text{II.12})$$

The propagation constant is given by [25]:

$$\beta = \frac{2\pi}{\lambda_g} \quad (\text{II.13})$$

the phase velocity is given by [25]:

$$v_p = \frac{\omega}{\beta} = \frac{c}{\sqrt{\epsilon_{\text{eff}}}} \quad (\text{II.14})$$

where

c: speed of the light ($c = 3 \times 10^8 \text{ m/s}$ in free space)

The electrical length θ for any given physical length of a microstrip is as follows [4]:

$$\theta = \beta \ell \quad (\text{II.15})$$

where ℓ is a physical length of the microstrip.

II.5 Loss in microstrip

There is a loss in microstrip that is commonly occurs under filter design. The approximation expressions of the loss are hard to extract and quantify, so in some cases losses can be neglected for design purposes.

II.5.1 Conductor loss

The losses in microstrip circuits arise from conductor loss due to resistive losses in the strip and it is a primary loss mechanism at low frequencies. The skin depth is a layer that is conducting a current, for a common metal such as Aluminum and Copper the skin depth is about 0.8 μm at 10 GHz. As the surface roughness increases, the current path increases and the conductor loss increases. And the conclusions are smooth substrates are essential for long circuits at high microwave and millimeter wave frequencies.

II.5.2 Dielectric loss

It is due to the polarization heating by time-varying fields in the substrate and radiation due to the antenna action of the microstrip. Because of reversal polarization losses in the substrate, the dielectric loss arises and the measure of this loss mechanism is the loss tangent.

II.5.3 Radiation loss

Open stub, bends and discontinuities on transmission line excite higher-order modes and cause the radiation of energy. The stub becomes a significant percentage of wavelength and experience as an antenna.

II.6 Microstrip discontinuities

All practical microstrip circuits contain discontinuities. The discontinuities include the bends, the width changes, the open ends, the gaps and T-junctions. Although such discontinuities give rise to only very small capacitances and inductances (often <0.1 pF and 0.1 nH) the reactance of these become particularly significant at the high microwave and into millimeter wave frequencies [26].

II.6.1 Main discontinuities

Some types of microstrip discontinuities are as follow:

II.6.1.1 bend

Right-angle bends of microstrips may be modelled by an equivalent T-network, as shown in Figure II.2. (Kupta and al., 1996) have given closed-form expressions for evaluation of capacitance and inductance [4].

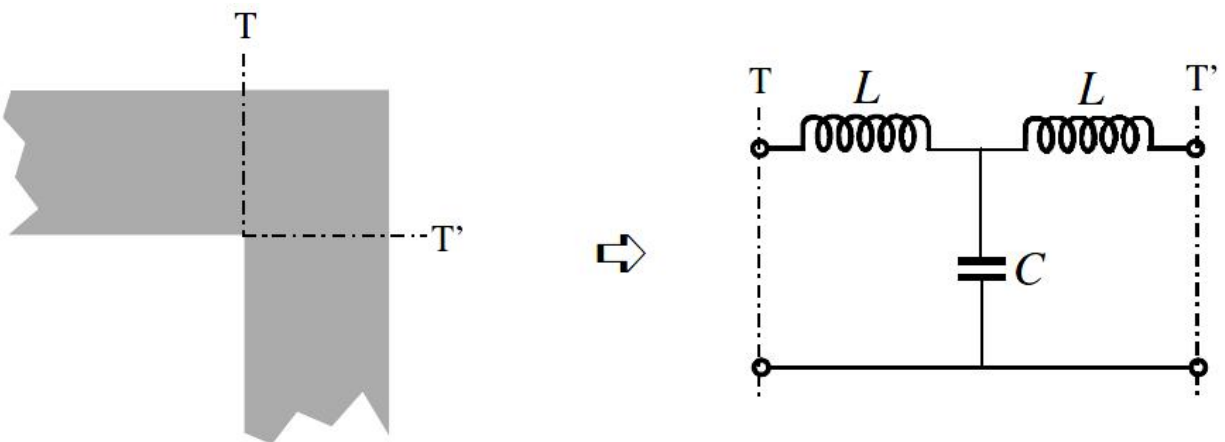


Figure II.2 Microstrip discontinuities bends and its equivalent circuit [27].

II.6.1.2 steps in width

For symmetrical microstrip step, the capacitance and inductances of the equivalent circuit indicated in Figure II.3 may be approximated by the following formulation [28].

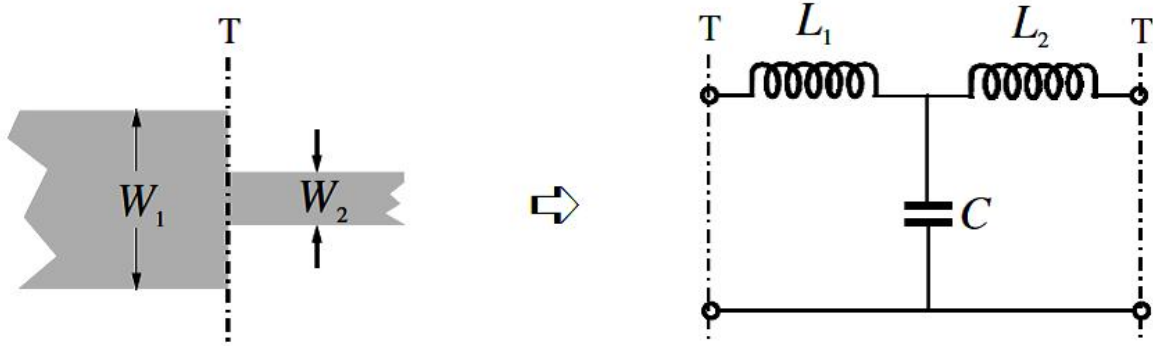


Figure II.3 Symmetrical microstrip steps and its equivalent circuit[1].

$$C = 0.00137h \frac{\sqrt{\epsilon_{eff1}}}{Z_{01}} \left(1 - \frac{w_2}{w_1}\right) \left(\frac{\epsilon_{eff1} + 0.3}{\epsilon_{eff1} - 0.258}\right) \left(\frac{\frac{w_1}{h} + 0.264}{\frac{w_1}{h} + 0.8}\right) \text{ (pF)} \quad (\text{II.16})$$

$$L_1(nH) = \frac{L_{w1}}{L_{w1} + L_{w2}} L \quad (\text{II.17})$$

and

$$L_2(nH) = \frac{L_{w2}}{L_{w1} + L_{w2}} L \quad (\text{II.18})$$

with

$$L_{wi} = Z_{ci} \sqrt{\frac{\epsilon_r}{C}} \quad (\text{II.19})$$

$$L = 0.000987h \left(1 - \frac{Z_{01}}{Z_{02}} \sqrt{\frac{\epsilon_{eff1}}{\epsilon_{eff2}}}\right)^2 \text{ (nH)} \quad (\text{II.20})$$

Where L_{wi} for $i= 1, 2$ are the inductances per unit length of the microstrip having widths w_1 and w_2 respectively. While Z_{0i} and ϵ_{effi} denote the characteristic impedance and effective dielectric constant corresponding to width w_i .

c : is the light velocity in free space. h : is the substrate thickness in micrometers.

II.6.1.3 Open ends

At the open end of a microstrip line with a width of w , the fields do not stop abruptly but extend slightly further due to the effect of the fringing field. This effect can be modeled either with an

equivalent shunt capacitance C_p or with an equivalent length of a transmission line Δl , as shown in Figure II.4 the equivalent length is usually more convenient for filter design.

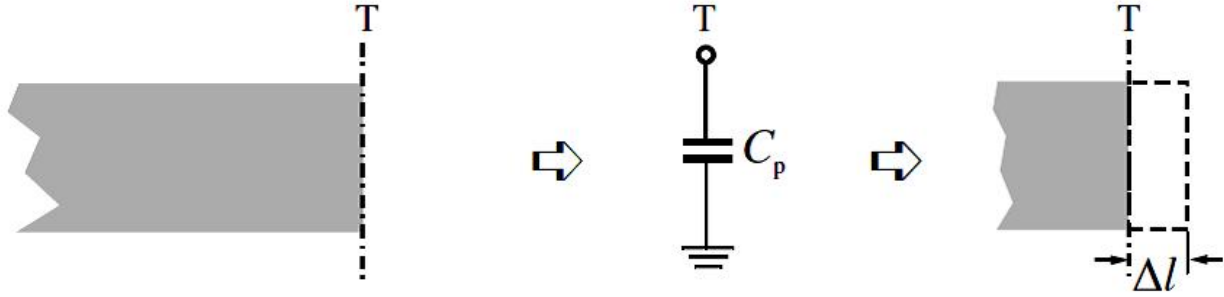


Figure II.4 Microstrip discontinuities open end[1].

The relation between the two equivalent parameters may be found by [28].

$$\Delta l = \frac{cZ_0C_p}{\sqrt{\epsilon_{\text{eff}}}} \quad (\text{II.21})$$

where c is the light velocity in free space, and a closed-form expression for $\frac{\Delta l}{h}$ is given as [28].

$$\frac{\Delta l}{h} = \frac{\xi_1 \xi_3 \xi_5}{\xi_4} \quad (\text{II.22})$$

where

$$\xi_1 = 0.434907 \frac{\epsilon_{\text{eff}}^{0.81} + 0.26 \left(\frac{w}{h}\right)^{0.8544} + 0.236}{\epsilon_{\text{eff}}^{0.81} - 0.189 - \left(\frac{w}{h}\right)^{0.8544} + 0.87} \quad (\text{II.23})$$

$$\xi_2 = 1 + \frac{\left(\frac{w}{h}\right)^{0.371}}{2.35\epsilon_r} \quad (\text{II.24})$$

$$\xi_3 = 1 + \frac{0.5274 \tan^{-1} \left(0.084 \left(\frac{w}{h}\right)^{\frac{1.9413}{\xi_2}} \right)}{\epsilon_{\text{eff}}^{0.9236}} \quad (\text{II.25})$$

$$\xi_4 = 1 + 0.037 \tan^{-1} \left(0.067 \left(\frac{w}{h}\right)^{1.456} \right) \{6 - 5 \exp[0.036(1 - \epsilon_r)]\} \quad (\text{II.26})$$

$$\xi_5 = 1 - 0.218 \exp \left(-7.5 \frac{w}{h} \right) \quad (\text{II.27})$$

The accuracy is better than 0.2% for the range of $0.01 \leq \frac{w}{h} \leq 100$ and $\epsilon_r \leq 128$.

II.7 S-parameters

The S-parameters is the most used parameters to describe an electrical network because it is difficult to obtain voltages and currents at high frequencies. For Z and Y –parameters it is

necessary to use open and short circuit which at microwave frequencies may cause instability when active elements are involved[29].

In order to simplify the analysis of an RF circuit, the system can be defined as a two-port system as shown in Figure II.5.

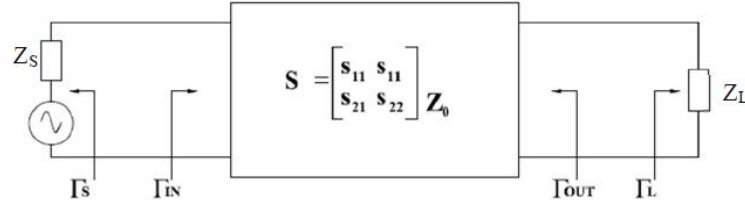


Figure II.5 General two-port network S-parameters[29].

The parameters shown in the figure I.5 are defined as follow

$$\Gamma_{IN} = \frac{S_{11} - \Delta \Gamma_L}{1 - S_{22} \Gamma_L} \quad \text{and} \quad \Gamma_{OUT} = \frac{S_{22} - \Delta \Gamma_S}{1 - S_{11} \Gamma_S} \quad (\text{II.28})$$

$$\Gamma_S = \frac{Z_S - Z_0}{Z_S + Z_0} \quad \text{and} \quad \Gamma_L = \frac{Z_L - Z_0}{Z_L + Z_0} \quad (\text{II.29})$$

where

$$\Delta = S_{11} S_{22} - S_{12} S_{21} \quad (\text{II.30})$$

- Δ is called the determinant of the S-parameter matrix.
- S_{11} is the input port reflection coefficient.
- S_{12} is the reverse transmission (insertion) gain.
- S_{21} is the forward transmission (insertion) gain.
- S_{22} is the output port reflection coefficient.

For some components and circuits, the scattering parameters can be calculated using network analysis techniques. Otherwise, the scattering parameters can be measured directly with a vector network analyzer (VNA) for one or two-port microwave network.

CHAPTER III

Design and Simulation of a novel LPF structure

III.1 Introduction

The purpose of this work is to design and simulate a novel microstrip LPF with high performance (low insertion-loss in the pass-band, high rejection band and sharpness response at the cutoff frequency) using a DGS technique. The numerical and EM simulations are carried out using MATLAB and zeland IE3D software [AppendixA] and [AppendixB]. The proposed filter is simulated on FR4 substrate with $\epsilon_r = 4.3$, $h = 1.62\text{mm}$ and $\tan\theta = 0.017$.

III.2 Design procedure of the proposed LPF

To design such a filter, different steps will be considered. First, a comparative study of some DGS units such as coupled C-shaped DGS unit, dumbbell DGS unit and square DGS unit is investigated. The layouts of the considered three DGS units are shown in Figure III.1 where Table III.1 illustrates their dimensions.

Coupled C- DGS unit	$a_1 = 1.7\text{ mm}$, $a = 1.1\text{mm}$, $b_1 = 4.2\text{mm}$, $b = 3\text{mm}$, $w = 0.6\text{mm}$, $s = 0.4\text{mm}$, $w_0 = 3.17\text{mm}$.
Dumbbell DGS unit	$a_2 = 0.55\text{ mm}$
Square DGS unit	$c = 9.2\text{ mm}$

Table III.1. Dimensions of the DGS units

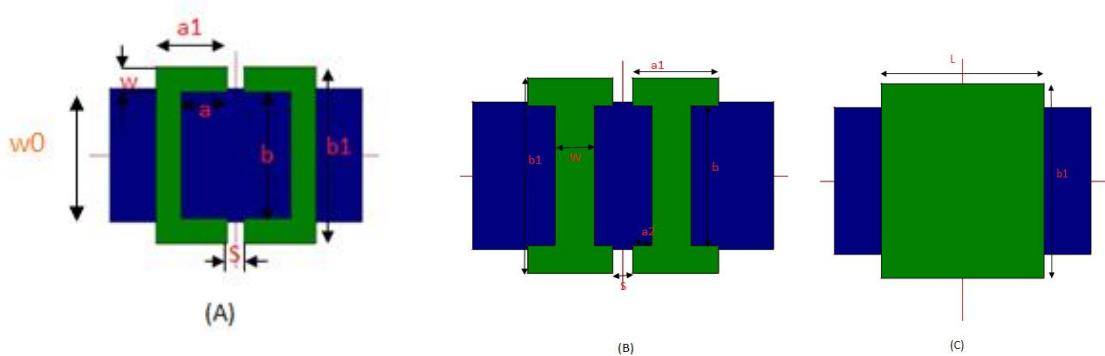


Figure III.1 The layout of the three DGS units

(a) C-DGS, (b) Dumbbell, (c) Square.

The simulated S-parameters of the three DGS units are shown in the Figure III.2 where the x-axis represents the Frequency in GHz and the y-axis represents the Magnitudes of S-parameters in dB.

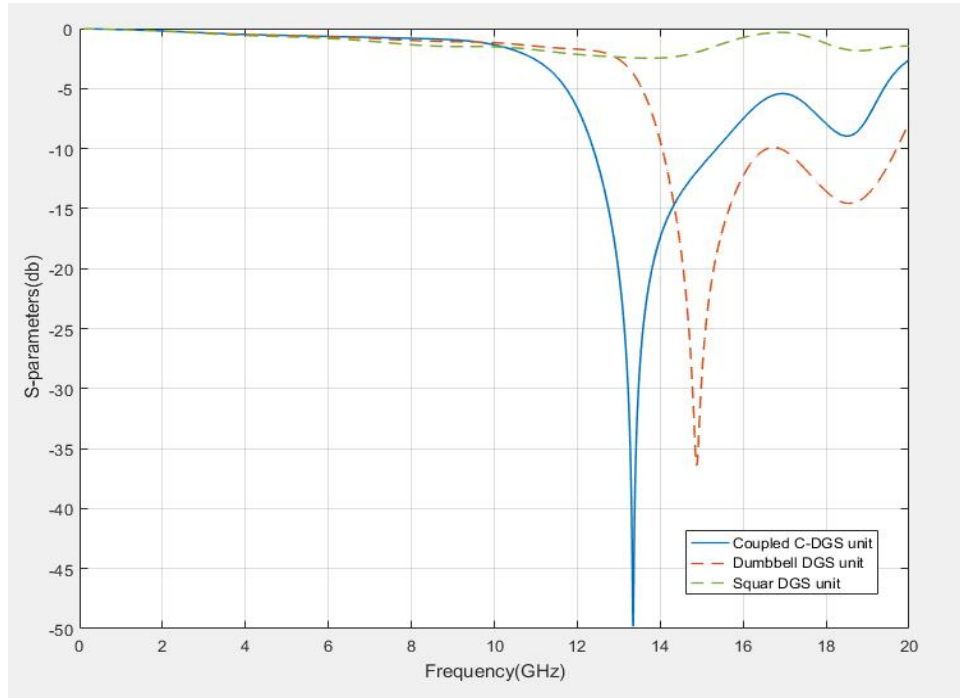


Figure III.2. The simulated S-parameters of the three DGS units.

From Figure III.2, it is observed that the dumbbell DGS unit has a stop-band response of less than 10-dB from 14.2 GHz to 16.8 GHz. The biggest stop-band from 12.38 GHz to 15.35 GHz is formed by the coupled C. Hence, the coupled C- DGS unit has wider stop-band than the dumbbell and square DGS units.

From the previous discussion, it is shown that the coupled C-DGS unit is more appropriate in designing LPF with a wide rejection band. Therefore, to enhance this type of band, at least two symmetrical and/or asymmetrical DGS units should be cascaded [30]. This type of structure is called periodic DGS units. In this study, we will start by designing an LPF with small size, wide and deep stop-band rejection based on the non-uniform cascaded coupled C-DGS unit as shown in Figure III.3. The considered dimensions are $b_3 = 4.8 \text{ mm}$, $b_2 = 3.6 \text{ mm}$, $s = 0.4 \text{ mm}$ separated by distance $d_1 = 12.2 \text{ mm}$ and $d_2 = 1.8 \text{ mm}$. The simulated results are shown in Figure III.4.

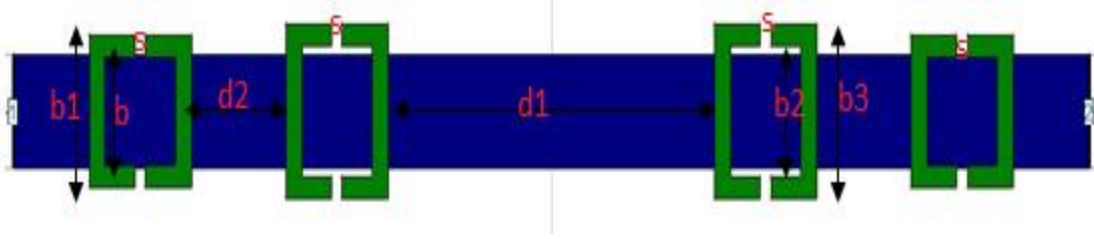


Figure III.3. Geometry of the LPF

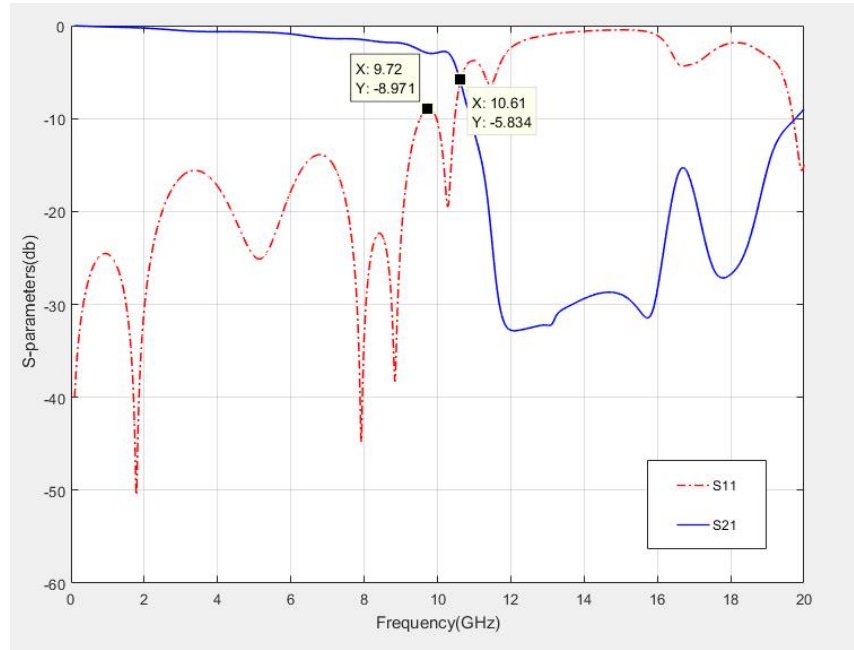


Figure III.4. S-parameters results.

The simulated S-parameters S21 and S11 show an LPF with a cutoff frequency of 10.61 GHz, and wide rejection band which is not deep enough. In what follows, some important modifications will be introduced to the structure so that to enhance band and wide rejection band. For that, we will propose a modified LPF with mirrored series-resonant branch loaded by radial stubs. In what follows, the design procedure is described.

- **Step1:** LPF using open-circuited stub is designed as shown in Figure III.5(a) with parameters $w_1=0.3$ mm, $w_2 = 5.5$ mm, $L_1 = 10.25$ mm and $L_2 = 1.8$ mm.

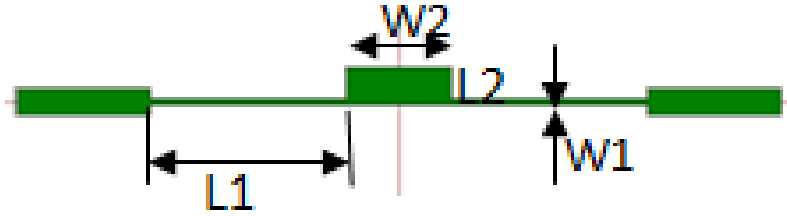


Figure III.5(a) LPF using open-circuited stub

- **Step 2:** In order to excite a transmission zero, two slots with the length of $L3=2.45\text{mm}$ and width of $W3=0.9\text{mm}$ are etched inside the open-circuit as shown in Figure III.5(b).

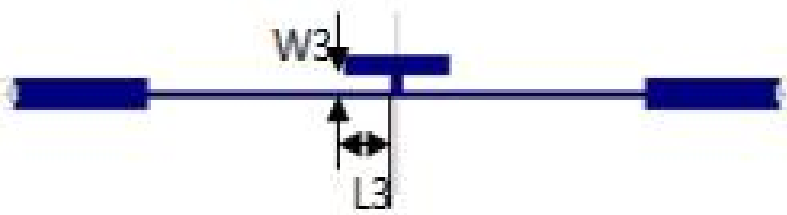


Figure III.5(b) Series-resonant branch

- **Step 3:** To improve the selectivity, a radial stub ($R2= 4.69\text{mm}$, $R1= 1.8\text{mm}$ and the angle is around 17.9°) is added at the terminal of the series resonant branch, as depicted in Figure III.5(c), so that to move the transmission zero toward 3-dB cutoff frequency.

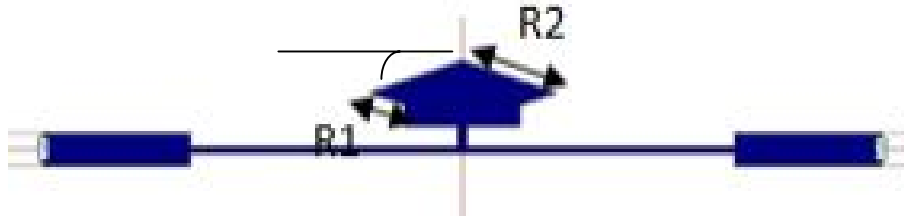


Figure III.5(c) Series-resonant branch loaded by radial stub

- **Step 4:** At the end, a mirrored structure of the series-resonant branch loaded by radial stub is added as shown in Figure III.5(c).



Figure III.5(d) Mirrored structure.

The simulation results of the four steps are shown in Figure III.6.

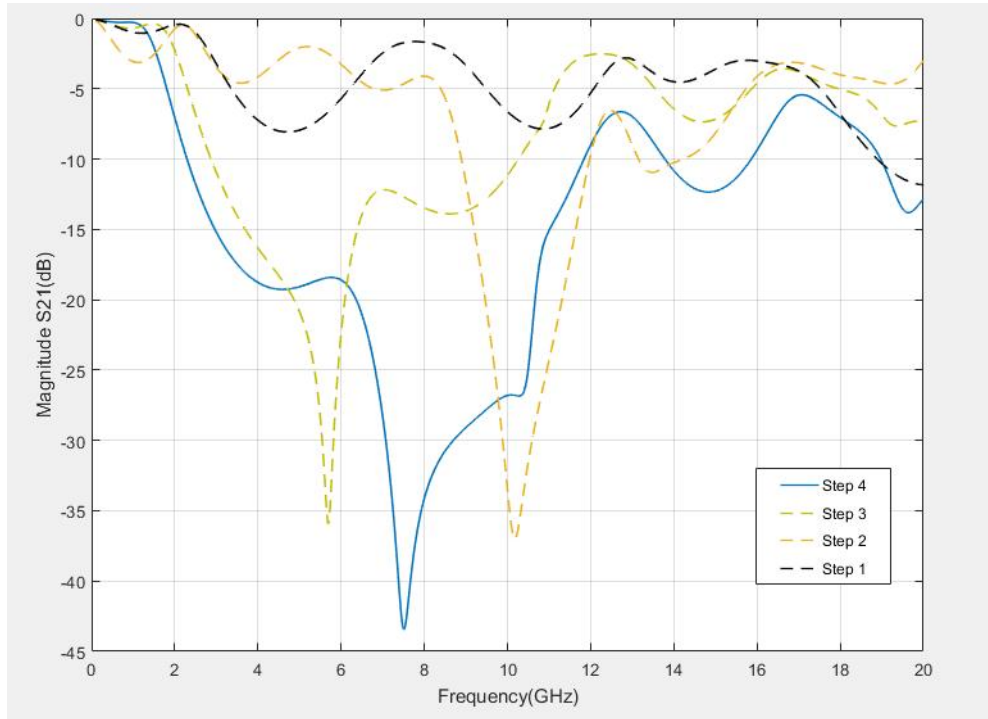


Figure III.6 The magnitude of S21 for four steps.

By using the mirrored series-resonant branch loaded by radial stub, an LPF with 3-dB cutoff frequency of 1.4GHz and wide rejection band starting from 3.62 to more than 10GHz is achieved. However, both the stop band and the sharpness still need improvement. For that, coupled C-DGS units are added to enhance the LPF performance as shown in Figure III.7 where Figure III.8 depicts the simulation results.

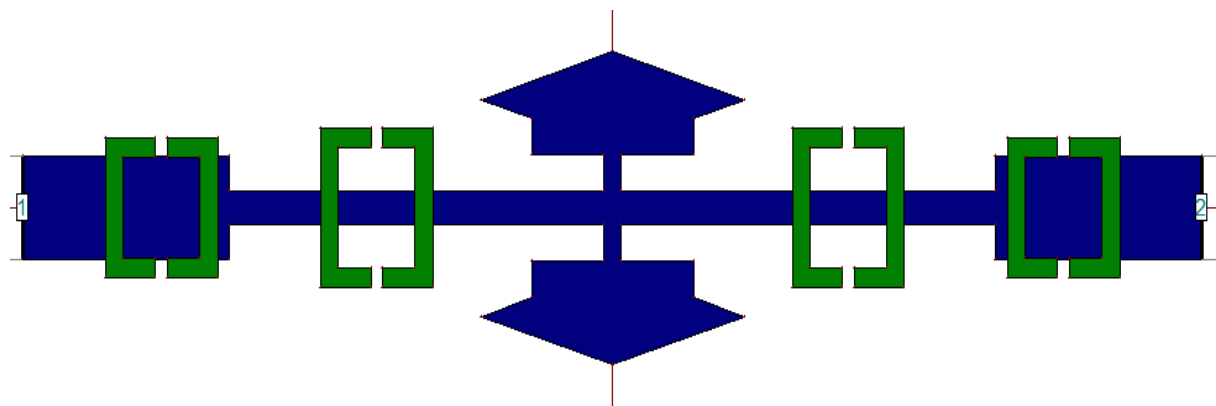


Figure III.7 Mirrored series-resonant branch with coupled C-DGS.

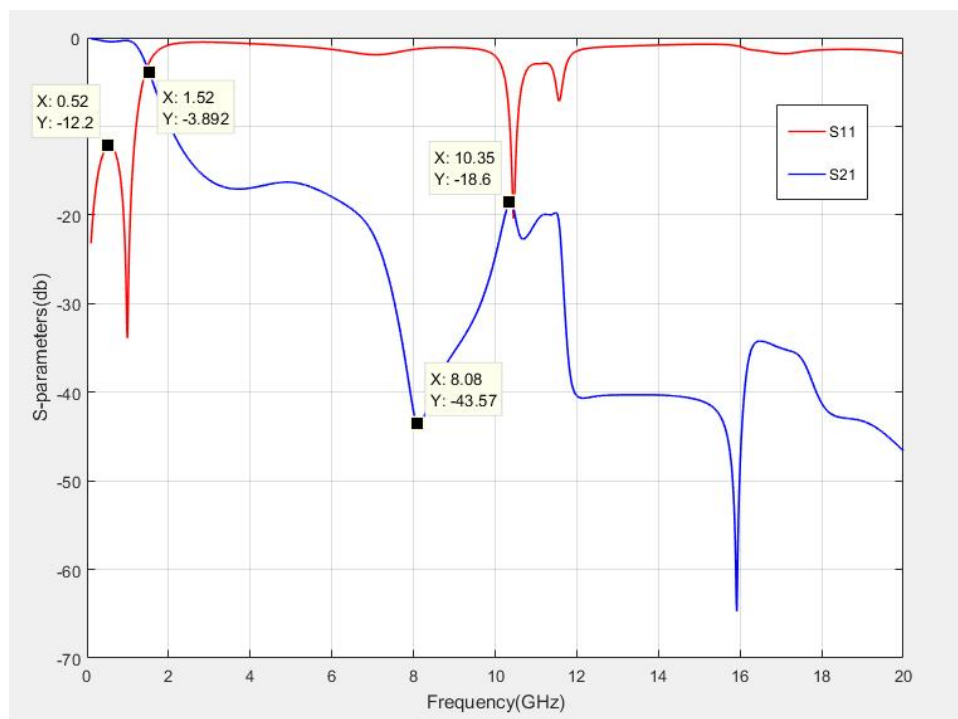


Figure III.8 Simulation results of the proposed LPF based on Mirrored series-resonant branch along with coupled C-DGS

From Figure III.8, it is noticed that adding coupled C-DGS units enhance the LPF characteristics where the cutoff frequency of 1.52 GHz, the return loss of 12.2 dB and the maximum magnitude of S21 is around 43.57 dB.

A comparison result between the filter structure without and with DGS units is summarized in Table III.2.

	Without C-DGS	With C-DGS
Cutoff frequency (f_c) in GHz	1.65	1.52
The insertion loss in dB	<0.94	<0.22
Maximum magnitude of S21 in dB	42.5	43.57
Return loss in dB	-16.02	-12.2
Stop-band (GHz) at 15 dB rejection	from 3.62 to 10.90	from 2.63 more than 20

Table III.2. A comparison result between the filter structure without and with DGS units

In order to reach an LPF with high performance, high impedance lines loaded by radial stub are added as shown in Figure III.9. The considered parameters are: $L_4 = 7.85$ mm, $L_5 = 2.55$ mm, $L_6 = 11.4$ mm, $d_4 = 3.39$ mm, $d_5 = 0.9$ mm, $W_4 = 0.4$ mm, and the angle is about 17.9° .

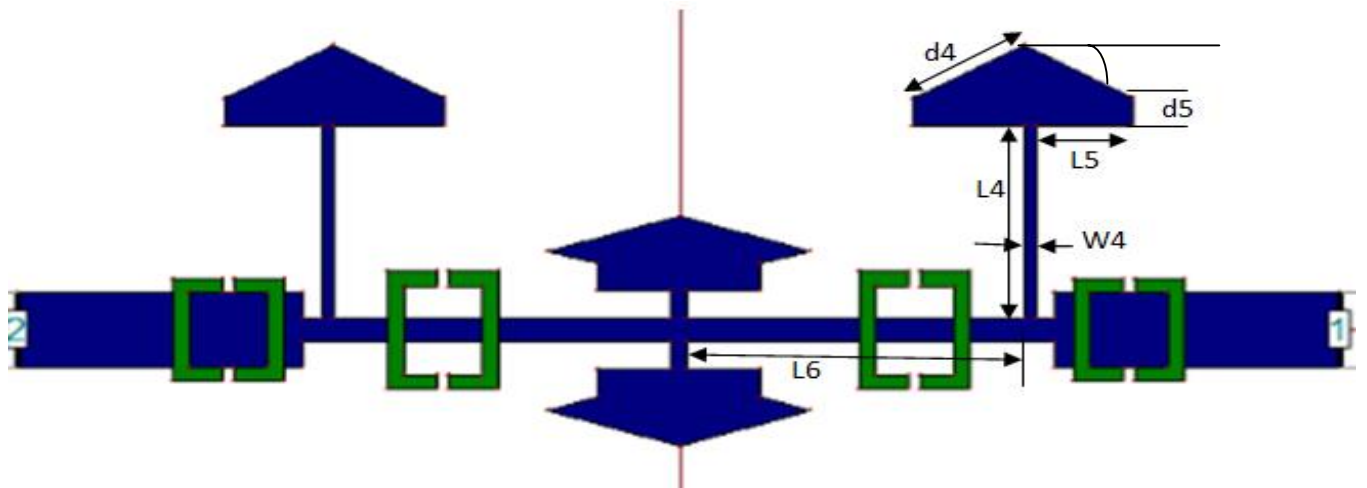


Figure III.9 Final geometrical structure of the proposed LPF

The following figure shows the S-parameters results of the final LPF structure.

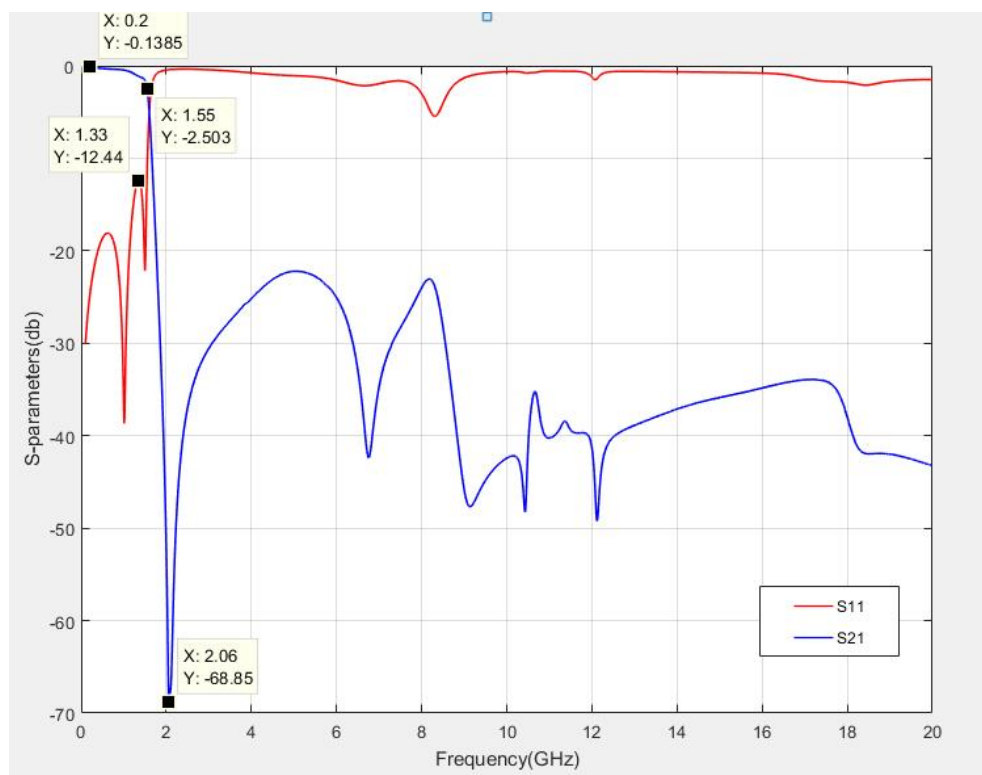


Figure III.10S-parameters results of the proposed final LPF structure.

From Figure III.10, it is clear that the filter performance has improved by using high impedance lines loaded by radial stubs.

The simulation results are summarized in Table III.3.

Cutoff frequency in GHz (f_c)	Insertion loss in dB	$S_{21\max}$ in dB	Return loss in dB	Stop-band (GHz) at 20-dB rejection in dB	Sharpness factor (SF)	Selectivity (ξ) in dB/GHz
1.55	<0.2	68.85	12.44	from 1.78 to more than 20	0.75	130

Table III.3. Simulation results

III.3 Implementation and Experimental Results

III.3.1 Implementation

The circuit fabrication was done using vector network analyzer machine shown in Figure III.11 whereas the photographs of the fabricated filters are shown in Figures III.12.

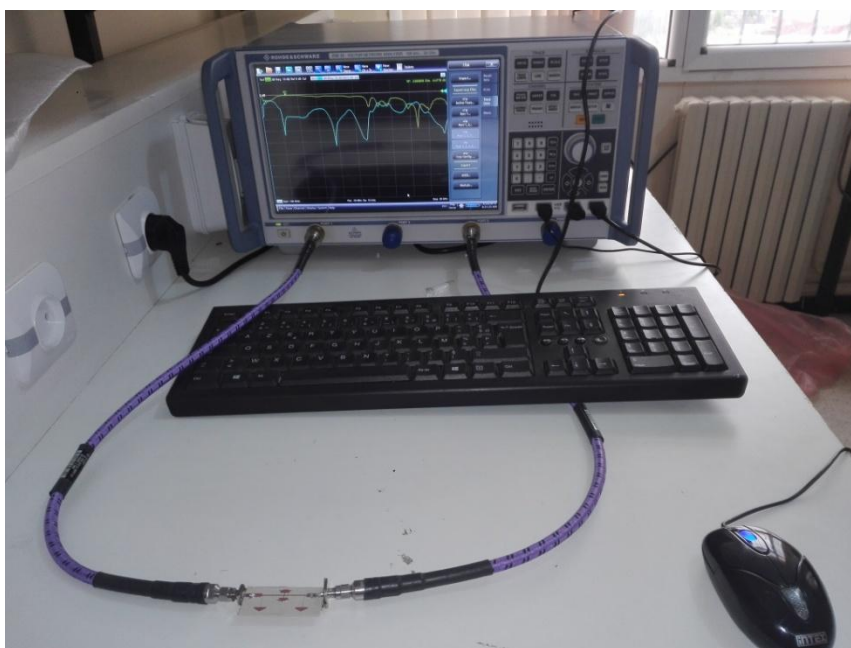


Figure III. 11 Vector network analyzer.

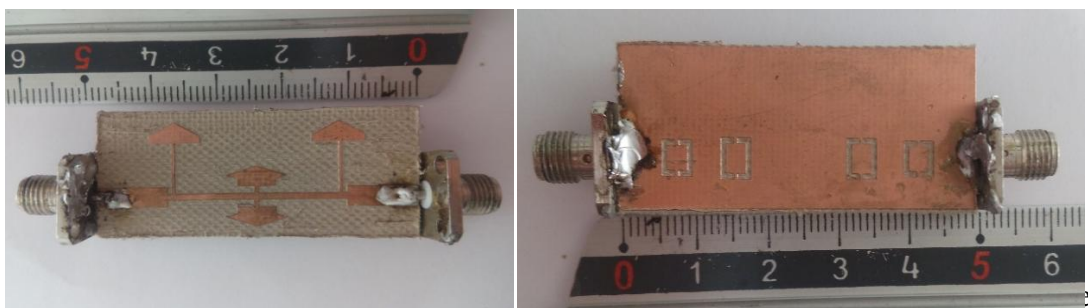


Figure III. 12 Photography of the fabricated of the final structure Top and Bottom view respectively.

III.3.2. Experimental Results

After the fabrication process, the filters performances are measured by using a Rohde & Schwarz VNA .Figure III.13 and Figure III.14 shown the S-parameters measured/simulated results of the final structure low pass filters.

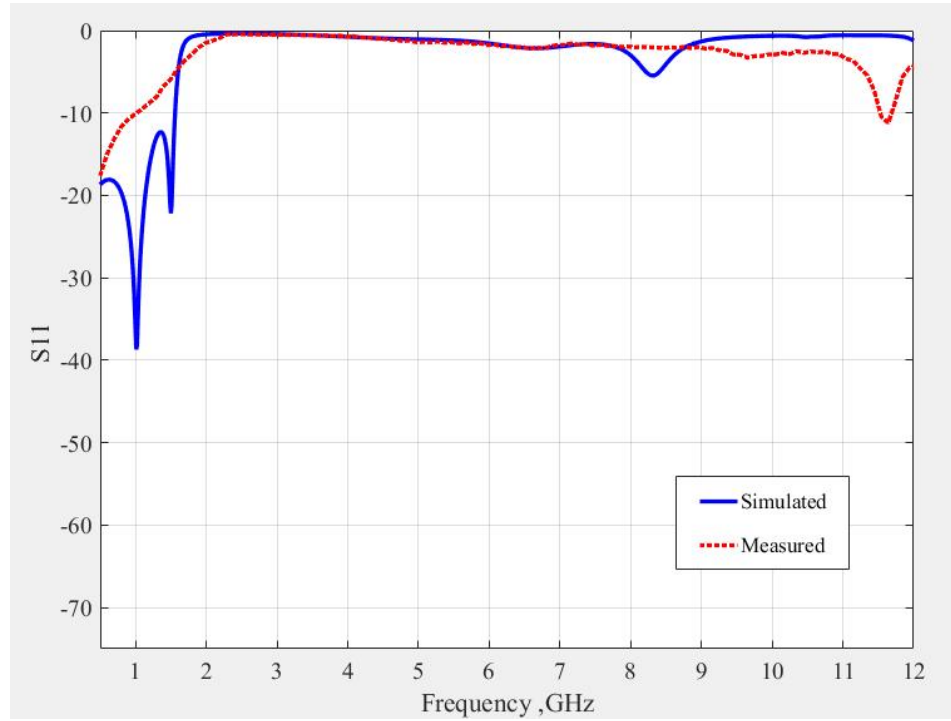


Figure III. 13 Measured and simulated S_{11} of the final structure LPF.

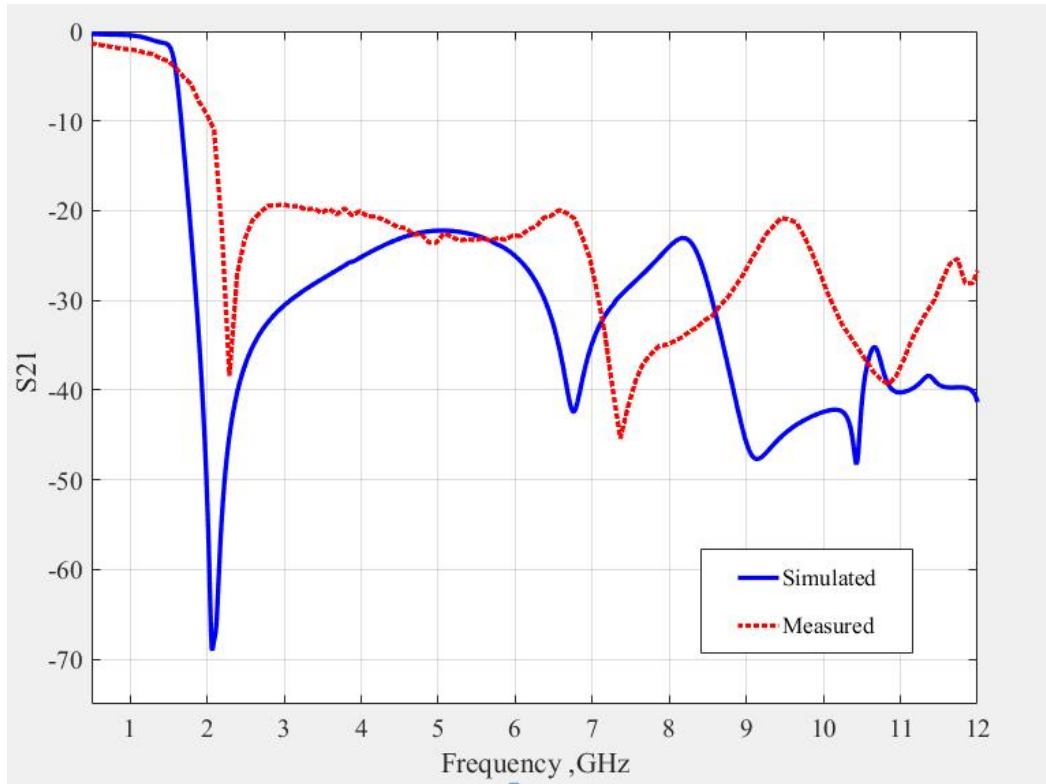


Figure III. 13 Measured and simulated S21 of the final structure LPF.

The results exhibit an acceptable agreement between the measurement and simulation results. due to the available substrate material which is not suitable for more than C-band applications. Moreover, this degradation is most probably attributed to the tolerance in fabrication process, diversity of material parameters and additional insertion loss. Despite this small fluctuation, the filters still present satisfactory performance and meet the requirements.

The performance comparison of the proposed LPF with some other LPFs is illustrated in Table III.4. It is clear from Table III.4 that the presented LPF offers much wider rejection level (lower than 20 dB) from 1.78 to more than 20 dB. It can be seen from Table III.4 that the proposed filter provides good performances in stopband rejection, passband return loss and those reported in the literature.

	Ref. [31]	Ref. [32]	Thiswork
Substrate dielectric constant/height (mm)	1.52/1.524	2.65/0.93	4.3/1.62
Cutoff frequency(f_c) inGHz	1.688	3.62	1.55
Stop-band (GHz)at 20 dB rejection	from 2.22 to 7.12	from 5.1 to more than 20	from 1.78 to more than 20
Pass-band insertionloss(dB)	–	< 0.1	< 0.2
Pass-band return loss (dB)	–	17.1	12.44

Table III.4.Comparison of the proposed DGS-LPF with other existing LPFs.

III.4 Conclusion

In this chapter, a new structure of low pass filter (LPF) using mirrored series-resonant branch and DGS techniques is introduced. The proposed LPF have shown satisfactory results in terms of wide rejection band (from 1.78 dB to more than 20 dB), sharp selectivity (SF of 0.75), selectivity ξ of 130 dB/GHz and low insertion loss in the pass-band.

General Conclusion

In this work, a novel LPF has been designed and optimized using the electromagnetic (EM) simulation IE3D software. Furthermore, the filter's performances have been compared to those reported in literature.

This work has been organized as follows:

A literature review of microwave filters and discussion about the DGS techniques have been introduced in the first Chapter. The second Chapter dealt with the microstrip transmission line theory. In the last chapter, a design of an LPF with broad rejection band, low insertion loss, sharpness response and compact size has been introduced. Moreover, in the same chapter, results, discussions and comparisons with the previous published works have been presented.

It has shown that the proposed LPF had successfully produced the wide rejection in the stop-band, extremely low insertion loss, good return loss and compact size.

As further work, the following points are suggested:

1. It would be interesting to fabricate and measure the designed LPF.
2. Investigation on the new types of LPF and evaluate their performances.
3. The creation of a new DGS design.

Finally, we hope that this work will be beneficial for further microwave projects in general and for filter applications in particular.

References

- [1] S. Boudaa, M. Challal and R. Mehani, "Miniaturized Microstrip Ultra-Wide Stopband Low Pass Filter Design," The 4th International Conference on Electrical Engineering–ICEE'2015, 13-15 December 2015, Boumerdes, Algeria. DOI:10.1109/INTEE.2015.7416715, Publisher: IEEE.
- [2] David M. Pozar, "Microwave Engineering," - ISBN 978-0-470-63155-3 - Copyright © 2012 by John Wiley & Sons, Inc.
- [3] Nadia Benabdallah, Nasreddine benahmed, Fethi Tarik Bendimerad, "Analysis and Design of an UWB Band pass Filter with Improved Upper Stop Band Performances, " International Journal of Modern Engineering Research (IJMER) ISSN: 2249-6645 -2013.
- [4] Jia-Sheng hong M. J. Lancaster, "Microstrip **Filters for RF/Microwave Applications**," -ISBN 0-471-22161-9- Copyright © 2001 by John Wiley & Sons.
- [5] Randall W. Rhea H.Badr El-Din and A. El-Shaarawy, "**Structures electromagnetiques a bandes interdites pour des applications de filter** ", Toulouse University, 17 December 2009, pp.66-74.
- [6] M.-H. Weng, C.-Y. Hung, and H.-W. Wu, "A **novel compact dual-band band-pass filter using dual-mode resonators**," IEICE Trans. Electron., E88-C, No. 1, pp. 146-148, January 2005.
- [7] Standards Coordinating Committee, "IEEE **Standard for Microwave Filter Definitions**," -ISBN 978-0-7381-6635-3- Copyright © 20 may 2011 by IEEE.
- [8] http://www.electronics-tutorials.ws/filter/filter_3.html
- [9] G. L. Matthaei, L.Young and E. M. T. Jones, Microwave Filters, Impedance-Matching Networks and Coupling Structures. Norwood, MA : Artech House, 1980.
- [10] D. M. Pozar, Microwave Engineering.^{3rd} edition, John Wiley and Sons, Inc. New York, 1998.
- [11] F. T. Ulaby, R. K. Moore, and A. K. Fung, Microwave Remote Sensing: Active and Passive,

Volume I, Microwave Remote Sensing, Fundamentals and Radiometry. Addison-Wesley, Reading, Mass., 1981.

[12] F. E. Gardiol, Introduction to Microwaves, Artech House, Dedham, Mass., 1984.

[13] M.A Bousmaha, "Analyse et conception de nouvelles structures de filtres larges bandes pour des applications en Télécommunications", Magister thesis, laboratoire LTT, Faculty of Technology, Abou Bakr Belkaid University, TLEMCEM, Algeria, 2011, 180 p.

[14] Lim, J. S, C. S. Kim, Y. T. Lee, "A spiral-shaped defected ground structure for coplanar waveguide", IEEE Microwave Compon. Lett, Vol. 12, No.9, 2002, pp. 330 - 332.

[15] Chen, J. X., J. L. Li, K. C. Wan, "Compact quasi-elliptic function filter based on defected ground structure", IEE Proc. Microwaves Antennas Propagation, Cambridge University Press and the European Microwave Association, Vol. 153, No.4, 2006, pp. 320 - 324.

[16] H. Louazene, "Design, Development and Optimization Ultra-Wideband - Pass Filters bands for Wireless Communication Systems ", Magister thesis, Faculty of New Technologies of Information and Communication, UKMO, Algeria, 08 June 2014, 94p.

[17] C. Insik and L. Bomson, "Design of defected ground structures for harmonic control of active microstrip antenna," IEEE Antennas Propag. Soc. Int. Symp., Vol. 2, pp. 852–855.

[18] M. Challal, A. Boutejdar, M. Dehmas, A. Azrar and A. Omar "Compact Microstrip Low-Pass Filter Design with Ultra-Wide Reject Band using a Novel Quarter-Circle DGS Shape, " ACES Journal- The Applied Computational Electromagnetics Society, vol. 27, n° 10, pp. 808-815, Oct. 2012..

[19] A. K. Arya, M. V. Kavtikeyan, A. Patnaik "Defected Ground Structure in perspective of microstrip antenna" frequenz journal Vol 164.pp. 5-6, 2010.

[20] L. H. Weng, Y. C. Guo, X. W. Shi, "An overview on defected ground structure", National Key Laboratory of Antenna and Microwave Technology, Indian University Progress In Electromagnetics Research B, Vol. 7, 2008, pp. 173 - 189.

[21] L. G. Maloratsky, "Passive RF and Microwave Integrated Circuits", Elsevier, USA, ISBN: 9780080492056, 1 st Edition, 2004, 368p.

[22] Y. Touati, F. Saidi, "Ultra Wide Bandpass Filters using Defected Ground Structure

- Technique ", Magister thesis, IGEE, University M'Hamed Bougara, Boumerdes, Algeria, 2012, 37p.
- [23] K. Chang, RF and Microwave Wireless Systems. John Wiley and Sons, Inc. New York, 2000.
- [24] T. K. Sarkar, R. Mailloux, A. A. Oliner, M. Salazar-Palma and D. L. Sengupta, History of Wireless, 2nd ed., NY, USA, John Wiley & Sons, INC., 2006.
- [25] Matthew N. O. Sadiku, "Elements of Electromagnetics", Oxford University Press, 2000.
- [26] C. Insik and L. Bomson, "Design of defected ground structures for harmonic control of active microstrip antenna", IEEE Antennas Propagation, Vol. 2, 2002, pp. 852 - 855.
- [27] D. M. Pozar, "Microwave Engineering", John Wiley & Sons, Inc. New York, 1998
- [28] <http://www.microwavejournal.com/articles/22570>.
- [29] Tzong-Lin Wu, "Microwave Filter Design: Transmission Lines and Components", course given in Department of Electrical Engineering National Taiwan University.
- [30] L. H. Weng, Y. C. Guo, X. W. Shi, and X. Q. Chen," An overview on defected ground structure", Progress In Electromagnetics Research B, Vol. 7, pp.173–189, 2008.
- [31] R. Mehani. S. Boudda "Miniaturized Microstrip Wide Rejection Band Low Pass Filter Design", Final Year Project Report Presented in Partial Fulfilment of the Requirements for the Degree of master.
- [32] Shaheen, M., et al., "Compact LPF design with low cutoff frequency using V-shaped DGS structure," International Journal of Electronics and Communication Engineering & Technology(IJECET), Vol. 6, No. 1, 1–7, January 2015.
- [33] T. Tang, B. Lin, "Ultra-Wideband Band Pass Filter Using Hybrid Microstrip Defected Ground Structure", faculty of Communications and Guidance Engineering, Taiwan, 24 September 2008, pp. 3085 - 3089.

Appendix N° A:

❖ Overview of IE3D Software

IE3D is a full wave, method of moments (MOM) based electromagnetic simulator for analyzing and optimizing planar and 3D structures in a multi-layer dielectric environment. It solves Maxwell's equation in integral form and its solutions include the wave effects, discontinuity effects, coupling effects and radiation effects. The simulated result includes S, Y, and Z-parameters, VSWR, RLC equivalent circuits, current field distribution, near and far field estimation, radiation pattern etc.

IE3D is an extremely useful tool in the design of MMICs, RFICs, RF printed circuits, Microstrip and wired RF Antennas, multilayer PCBs and IC interconnections.

Key Features

- ✓ IE3D Fast EM Design Kit for real-time full-wave EM tuning, optimization and synthesis.
- ✓ Multi-fold speed improvement and multi-CPU support for much improved efficiency.
- ✓ Equation-based schematic-layout editor with Boolean operations for easy and flexible geometry editing and parameterization.
- ✓ Lumped element equivalent circuit automatic extraction and optimization for convenient circuit designs.
- ✓ Improved integration into Microwave Office from Applied Wave Research.

Applications of IE3D

- ✓ RF circuits, LTCC circuits and RF ICs.
- ✓ Microwave, RF and wireless antennas.
- ✓ RFID tag antennas.
- ✓ HTS filters.
- ✓ Electronic packaging and signal integrity.
- ✓ Microwave circuits and MMICs.
- ✓ Many other low to high frequency structures.

Appendix B

MATLAB program script used in a comparative study of some DGS units

```
load coupledc.txt;
data3=coupled;
x3=data3(:,1);
y3=data3(:,2);
load dumbbell.txt;
data2=dumbbell;
x2=data2(:,1);
y2=data2(:,2);
load squar.txt;
data1=squar;
x1=data1(:,1);
y1=data1(:,2);
plot(x3,y3,x2,y2,x1,y1)
xlabel('frequency(GHz)');
ylabel('S-parameters');
grid;
```